

**FITTING EFFECTIVE DIFFUSION MODELS TO DATA  
ASSOCIATED WITH A “GLASSY POTENTIAL”: ESTIMATION,  
CLASSICAL INFERENCE PROCEDURES AND SOME HEURISTICS**

\*

CHRISTOPHER P. CALDERON <sup>†</sup>

**Abstract.** A variety of researchers [14, 25, 29] have successfully obtained the parameters of low dimensional diffusion models using the data that comes out of atomistic simulations. This naturally raises a variety of questions about efficient estimation, goodness-of-fit tests, and confidence interval estimation. The first part of this article uses maximum likelihood estimation (MLE) to obtain the parameters of a diffusion model from atomistic data. I address numerical issues associated with attempting to realize asymptotic statistics results with moderate sample sizes in the presence of exact and approximated transition densities. Approximate transition densities are used because the analytic solution of a transition density associated with a parametric diffusion model is often unknown. I am primarily interested in how well the deterministic transition density expansions of Ait-Sahalia capture the curvature of the transition density in (idealized) situations that occur when one carries out simulations in the presence of a “glassy” interaction potential. Accurate approximation of the curvature of the transition density is desirable because it can be used to quantify the goodness-of-fit of the model and to calculate asymptotic confidence intervals of the estimated parameters. The second part of this paper contributes a heuristic estimation technique for approximating a nonlinear diffusion model. A global nonlinear model is obtained by taking a batch of time series and applying simple local models to portions of the data. I demonstrate the technique on a diffusion model with a known transition density and on data generated by the Stochastic Simulation Algorithm [20].

**Key words.** Effective diffusion model, multiscale approximation, likelihood ratio expansion, piecewise polynomial SDE, quasi-maximum likelihood, stochastic process approximation

**AMS subject classifications.** 15A15, 15A09, 15A23

**1. Introduction.** Complicated systems are often approximated by overly simplified models. A significant research effort has gone into attempting to efficiently summarize the information contained in complicated atomistic simulation with low dimensional effective models [27, 25, 29, 14]. Atomistic simulations contain many observables, an effective diffusion model aims at representing the salient features of the data in the drift component of a stochastic differential equation (SDE) and lumping the effects of the neglected details into the noise term. The appeal of effective models stems from the fact that information contained in the effective models can easily and quickly be extracted by analytical methods or well-established numerical procedures. The idea being that the “truth” is contained in the atomistic simulation, but the computational load required to get the information is so large that the researcher has a difficult time exploring all of the process parameters under study.

It should be noted that estimation of effective models from atomistic simulations (multiscale modeling) differs substantially from the estimation task in finance or econometrics. In multiscale modeling, one often only desires a crude *approximate* dynamical model in order to summarize the information contained in the simulation. It is desirable to have the parameters of the proposed effective model demonstrate smooth dependencies on the parameters of the underlying atomistic simulation so that one can potentially interpolate and extrapolate estimated parameter values yielding a collection of effective models valid at different system conditions. Estimation asso-

---

\*This work was partially supported by a Ford Foundation/NRC Fellowship

<sup>†</sup>Department of Chemical Engineering, Princeton University, Princeton, New Jersey 08544 (ccaldero@princeton.edu).

ciated with multiscale modeling is “easier” because one has control of the (assumed physically meaningful) data generating process <sup>1</sup>. In this article, I evaluate tools recently developed by the finance/econometrics community in multiscale applications and develop an estimation strategy that can assist in making the general idea behind Kevrekidis’ “Equation Free” methods more practical in situations where the data can be reasonably approximated by a diffusion model.

Before one attempts to wrap effective models around the output of an atomistic simulation a variety of assumptions need to be made about the data and the parametric model. In this paper, I obtain parameter estimates from the classical parametric framework. That is, one uses a single family of functions (of specified functional form) for the drift and diffusion coefficient functions of the SDE (a “structural model” [22]) that depends only on a finite number of parameters. I make the following assumptions about the atomistic system and the parametric diffusion model:

- A small set of order parameters [30, 23] that accurately summarize the full atomistic system are identified and easily measurable. The term “order parameter” is used to refer to the observables modelled in the effective diffusion SDE
- The parametric model is uniquely identifiable
- The *exact* transition density of the parametric model has all of the regularity properties that make MLE attractive. Namely it is the *asymptotically* most efficient estimator in the sense that the properly normalized parameter distribution associated with the procedure converges to a normal distribution with the smallest asymptotic variance (in the “nonergodic” this assumption is relaxed)
- The true parameter value admits a contiguous neighborhood and the process allows for a quadratic expansion of the likelihood ratio <sup>2</sup>
- The dynamics of the order parameters can be adequately described by a diffusion SDE
- The drift and diffusion coefficient of the effective SDE are suitably smooth (to be more specific assume the functions are infinitely differentiable with respect to the parameters and state, but this can be relaxed substantially) and the drift component of the SDE comes from the gradient of an effective potential [14, 29]. Even if the order parameter being considered is governed by a glassy potential (this term is described in section 2), a smooth drift coefficient function can be used to summarize key features of the free energy landscape <sup>3</sup>

The first item is extremely important and is an active area of research in our group [30], but will not be addressed in this article. The next two assumptions allow one to

---

<sup>1</sup>Sometimes one can bias (or “steer”) [25, 29, 23, 17] a batch of simulations to have a prescribed initial distribution of a certain observable. The biggest advantage one has in multiscale modeling is the ability to produce additional sample trajectories in order to reduce the variance of the parameter distribution. The laws governing the atomistic *simulation* do not change in contrast to the “laws” that govern financial institutions. The number of trajectories that can be used for estimation is only limited by the computational load required to carry out atomistic simulations. This author attributes Ioannis Kevrekidis for applying this concept to multiscale modeling.

<sup>2</sup>These terms are briefly introduced in section 4, consult van der Vaart [45] chapters 5-8 for a clear detailed treatment

<sup>3</sup>For example the global minimum value of the smooth effective free energy surface is the same as that of the more complicated glassy surface

trust the parameter estimates and allows one hope for checking if some asymptotic results associated with MLE [26, 45, 47] hold for the sample sizes used. The fourth item is briefly addressed in the final application of the second part of this paper where I estimate the parameters of a diffusion approximation of a jump process (the kinetic Monte Carlo model for the reduction of nitric oxide on a platinum surface given in [39] is revisited). The final issue is concerned with “model misspecification” [47], dealing with this issue is important if the effective model is to be of any practical use. I first obtain parameter estimates assuming the final item holds, but in section 4.3 classical techniques for testing this assumption *a posteriori* are outlined. Some nonparametric goodness of fit tests are better suited for practical implementation [11, 24], but classical tests are of interest because the tests used quantify how well a transition density approximation matches the curvature of the true density.

In order to use MLE one must have an approximation of the transition density of the diffusion process. Unfortunately, for many SDE’s the transition density is not available in closed-form so one must resort to some approximation of the density. In this paper, I am primarily concerned with using the Hermite expansions of Aït-Sahalia [2, 3] in some large sample statistics applications associated with various multiscale applications.

The remainder of this paper is organized as follows: Section 2 reviews the multiscale applications that this method aims at helping. Section 3 lays out the model systems used. Section 4 outlines the techniques and estimation tools used in the presence of “contaminated” <sup>4</sup> data and transition densities. Section 5 outlines a simple modeling procedure that can be used to study multiscale systems that satisfy the assumptions stated above. Section 6 contains the numerical results and discussion and the final section gives the conclusion and outlook.

**2. Motivation.** A situation encountered often in spin glasses [32], protein folding [23], and zeolites [9] is that of a harmonic “glassy” potential energy surface <sup>5</sup>. That is to say, when one looks at a free-energy surface from a distance, the shape of the free energy surface is roughly parabolic. When one looks closely at the details of the surface however, one sees many bumps in the surface (see figure 3.1). In many applications, it is believed that the order parameter of the process “funnels” its way down to the global minimum of the free energy surface [23] in the long time limit. Current computational power does not always allow one to carry out an atomistic simulation long enough to observe such a phenomena because the order parameter can get trapped in a local minima. Sometimes one can reach the global free energy minima by increasing the temperature parameter of the simulation [17, 12]. When this occurs, the force binding the order parameter to the global minimum still has a “bumpy” potential associated with it (but the magnitude of the bumps is smaller because of the new temperature scale). I refer to this hypothetical case as situation I.

Another commonly encountered scenario is one where the order parameter is

---

<sup>4</sup>This term is used to convey the fact that one knows that the true data does not follow the exact proposed parametric model

<sup>5</sup>This estimation strategy was developed in order to accurately measure the curvature of complicated free energy surfaces associated with atomistic simulations. If the location(s) of the dominant free energy wells are known by theory or simulation methods, then the estimation methods shown here can be used to measure the curvature at the well minima which can in turn be useful for getting information about transition pathways [13]. If one also has knowledge of where the saddles are and a protocol for starting meaningful simulations around the saddle point then the methods presented can also be used to determine the curvature of the unstable state points.

trapped in a free energy well which is not the global minimum of the surface. Many applications require system information at low temperatures, ruling out the simple technique mentioned in the previous paragraph. If the temperature of the system is so low that on the timescale of the atomistic simulation that the order parameter appears to be approximately bound by a smooth (but not necessarily harmonic) potential in a neighborhood of the local minima, then I will refer to this case as situation II.

Classic statistical mechanics models usually assume that the noise around the local minima is state independent. This assumption does not hold in a variety of interesting systems, [29, 14] so in all models I consider there is state dependent noise in the process. The estimation techniques presented in this paper deal with both situations described in the preceding paragraphs.

**3. Model Systems.** To idealize situation I and II, data is generated from two families of SDE's. This first family is meant to mimic situation I and has the form:

$$(3.1) \quad dX_t = \left( \kappa(\alpha - X_t) + \beta \sin((X_t - \alpha)\omega 2\pi) \right) dt + \sigma \sqrt{X_t} dW_t$$

The second family idealizes situation II and takes the form:

$$(3.2) \quad dX_t = \left( \kappa(\alpha - X_t) + 4\gamma(\alpha - X_t)^3 \right) dt + \sigma \sqrt{X_t} dW_t$$

Throughout the parameters are set to  $\alpha = 20$ ,  $\kappa = \sigma = 4$ , and  $\omega = \frac{1}{3}$ . The parameters  $\beta$  and  $\gamma$  take the values  $(0, 15, 60, 400)$  and  $(0, \frac{1}{400})$ . I refer to these cases as situations I A-D and situations II A-B respectively. The situation where  $\gamma$  and  $\beta$  are both zero is known as the Cox-Ingersoll-Ross (CIR) model and is one of the rare situations where an SDE with nonlinear coefficients has an explicit solution [2]. I use this example because it illustrates mean reversion, it demonstrates state dependent noise and most importantly has an exact closed-form transition density which can be used to help determine why a transition density approximation is failing.

Figures 3.1 and 3.2 plot the potential energy surfaces for the cases studied. In all cases, sample paths of the above processes are simulated using the explicit Euler scheme [28] with a step size  $\Delta t = 2^{-9}$  given data starting from the invariant density associated with situation I A. The data is observed every 16<sup>th</sup> step yielding a constant observation window spaced by  $\delta t_{obs} = 2^{-5}$  time units (in Situation I A-C the data is also sampled every 64<sup>th</sup> step giving  $\delta t_{obs} = 2^{-3}$ ). Each plot and graph that are grouped together in this paper used the same Brownian trajectories in order to simulate paths (the only difference between the sample paths is caused by the different drift coefficients) in order to reduce variation due to random number draws.

For the first part of this paper, the data generated by the SDE's above is modelled by the CIR class:

$$(3.3) \quad dX_t = \kappa(\alpha - X_t)dt + \sigma \sqrt{X_t} dW_t$$

For the second part of this paper, the following parametric family is used:

$$(3.4) \quad dX_t = \left( a + b(X_t - X_o) \right) dt + \left( c + d(X_t - X_o) \right) dW_t$$

Where  $X_o$  is user specified; the parameter vectors are estimated by techniques associated with maximum likelihood in all cases.

The second terms in the drift coefficient of the data generating processes are used to determine how robust the estimator is against model misspecification [47, 40, 8].

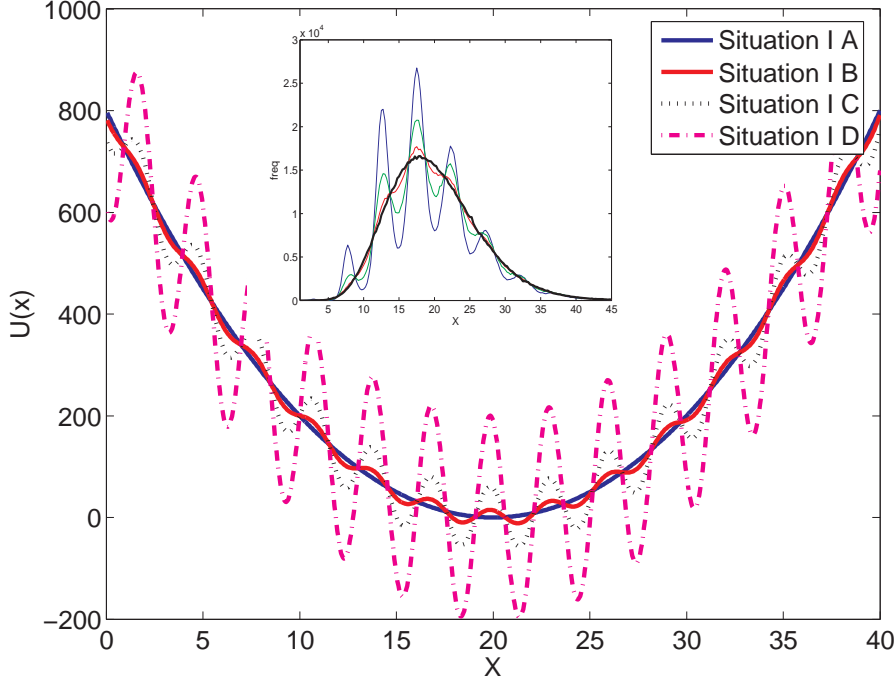


FIG. 3.1. *Situation I Potential* Potential energy function used to determine drift with  $\beta = (0, 15, 60, 400)$ . The inset shows the empirically measured invariant distribution for the four values of  $\beta$  used (with obvious correspondence between the 4 cases); the distributions are shown only to give one an idea of how the different parameter values affect the long-term dynamics (MLE parameters only depend on the observation frequency).

The perturbation terms are not modelled because it assumed their true (or approximate) functional form are completely unknown and the interest is primarily in the smooth noise and mean reversion parameters  $(\alpha, \kappa, \sigma)$ . Of course the presence of these extra terms affect the estimation of the parameters, it is shown in section 6 that the effects induced by these perturbation parameters affect things consistently with what a physicist or chemist would intuitively anticipate. The interesting feature demonstrated in the aforementioned section is quantitatively how the MLE procedure carried out with various transition density approximations respond to these perturbation parameters in relation to the exact transition density.

The reason for studying the first two idealized model systems stems from a desire to *carefully* numerically quantify how the MLE procedure with approximated transition density performs in tasks beyond point parameter estimation. The results obtained are of course specific to the model and parameter values used, however one can always obtain the parameters of a structural model from the particular system being studied and then carry out a similar “idealized” set of tests similar to the ones presented here by using established diffusion path simulation techniques [28].

The final model presented is a kinetic Monte Carlo simulation of nitric oxide (NO) reduction by hydrogen gas on a platinum (Pt) surface. The mechanism is as follows

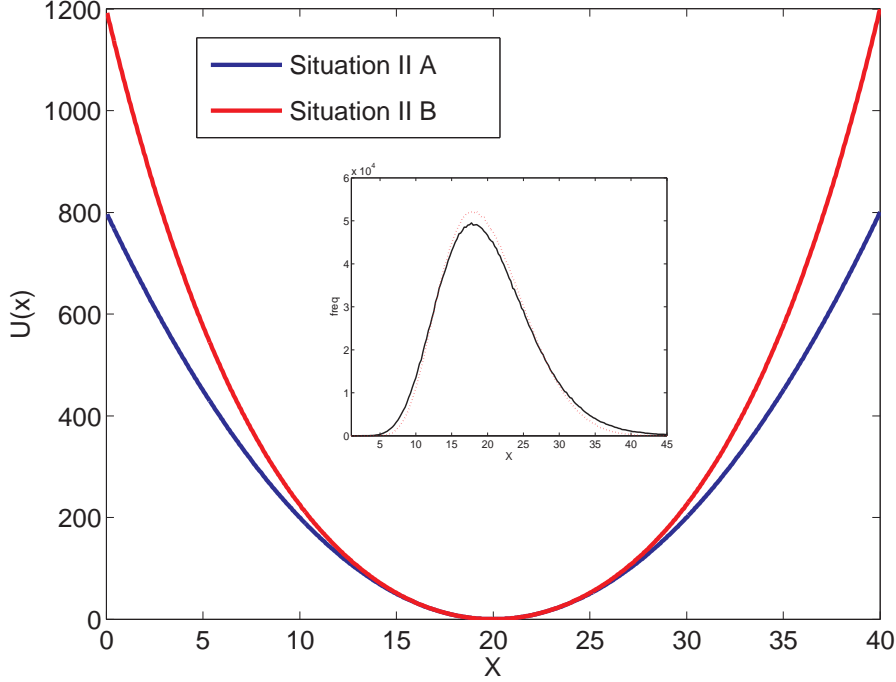
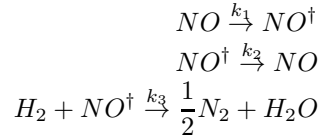


FIG. 3.2. *Situation II Potential* Potential energy function used to determine drift with ( $\gamma = 0, \frac{1}{400}$ ) along with inset of corresponding invariants distributions (the narrower distribution corresponds to the nonlinear perturbation case)

[44]:



(3.5)

$NO^\dagger$  represents NO absorbed onto the Pt surface; this mechanism is used with Gillespie's Stochastic Simulation Algorithm (SSA) [20] technique in order to construct stochastic evolution rules for the amount of  $NO$  in the system at any given time. This model is used because it exhibits nonlinear mean reversion with state dependent noise. The jump process is known to converge weakly to a diffusion with a cubic drift term as the system size parameter (denoted by  $N_{molecules}$ ) increases. This yields another "situation II" type scenario, but now the data generating process is not a genuine diffusion <sup>6</sup>. The parameter  $k_3$  is set to a numerical value of 4, the other model parameters used are given in [39]. In the final part of this paper the parameters of

<sup>6</sup>It should be pointed out that some approximations of the above process by a diffusion model [20] use as many Brownian driving terms as there are elementary reaction steps ; our black-box approach only uses one Brownian term for each state component (In this paper the noise contribution of the individual reaction events are lumped into a single noise term) .

the assumed model are extracted in the “small molecule” case ( $N_{molecules} = 3600$ ). This value is chosen because visual inspection indicates that the process has not yet converged to a diffusion (the observation frequency is the same as in the previous cases) with this parameter value, so the exact functional form of the diffusion model is unknown. A global estimate of the process is obtained using techniques presented in the second part of this paper and the invariant density of the obtained nonlinear diffusion model is compared to that of the actual SSA process in section 6.

**4. Statistical Tools.** In the beginning of this section, some classical statistical tools relevant to multiscale modeling are outlined. The tools are only briefly defined, references are given throughout which comprehensively describe the details of the theory applied. The tools below are applied to the estimation of the parameters of a stationary time series (the tools and theory in sections 4.1 and 4.4 are applied to a “nonergodic” time series <sup>7</sup> in section 6).

MLE’s importance <sup>8</sup> stems from the fact that one needs some kind of generic metric by which to judge a wide class of parametric models by. In situations where the underlying transition density satisfies a set of regularity assumptions [45] it is very appealing because it provides a consistent estimator with the minimum asymptotic variance. If one has a reliable estimates of the underlying transition density, then one can sometimes (in the stationary ergodic distribution case [26]) determine the asymptotic parameter distribution with a simple deterministic integral [22, 36]. One can also generate test statistics based on output of the MLE procedure which can be used to asses the goodness-of-fit of the parametric model [47].

Next, an optimal simple hypothesis test is introduced. Specifically, the transition density expansions are used in order to create the Neyman-Pearson test statistic [7]. A simple hypothesis test is useful when one wants to test the statistical significance of the magnitude of the changes in effective model parameters when one adds more features to the underlying atomistic simulation (e.g. one would like to determine if the changes in the effective model are significant when the parameters are estimated from the output of atomistic simulations that use a potential with and without electrostatic interactions).

It is already known that the simple models that are wrapped around the data do not faithfully represent the *exact* system dynamics. In section 4.3 methods that can be used to quantify how closely the proposed parametric models represent the data are reviewed. In section 4.4 a heuristic method that can be used in the nonergodic case for obtaining parameter uncertainty estimates is presented.

**4.1. Maximum Likelihood Basics.** The principal of maximum likelihood is based on maximizing the following integral with respect to the parameter  $\theta$ . In order to avoid technical complications, it is assumed throughout that the *exact* distribution of the process admits a density whose logarithm is well defined almost everywhere and the logarithm of the density is continuously twice differentiable and can be described by the proposed parametric family of distributions:

$$(4.1) \quad \int_{\Omega} f(\mathbf{x}; \theta) \log(f(\mathbf{x}; \theta)) d\Omega$$

---

<sup>7</sup>This term is intended to describe situations where the parameter distribution associated with an estimation scheme is not asymptotically normally distributed (with a deterministic covariance matrix); this can occur if the sample size is itself random or if the time series is nonstationary [5].

<sup>8</sup>In practice one usually deal with a quasi-maximum likelihood estimate. The difference between the two is described in section 4.3

In the above equation,  $\mathbb{Q}$  corresponds to the measure of the underlying probability space,  $f(\mathbf{x}; \theta)$  corresponds to the Radon-Nikodym derivative (consult [31, 47]) of the law of the random variable  $\mathbf{x}$  with respect to the underlying probability space and  $\mathbf{x}$  corresponds to a discretely sampled time series (of finite length =  $M$ ). Assume that if the measure of a set under  $\mathbb{Q}$  is zero it implies that the measure of the set under  $\mathbb{P}_\theta$  is also zero (the phrase “ $\mathbb{P}_\theta$  is absolutely continuous with respect to  $\mathbb{Q}$ ” is used to describe this situation). Let  $\mathbb{P}_\theta := \int \Omega f(\mathbf{x}; \theta) d\mathbb{Q}$ . For discrete Markovian models,  $f(\mathbf{x}; \theta)$  can readily be calculated by the following formula [22]:

$$(4.2) \quad f(\mathbf{x}; \theta) = f(\mathbf{x}_0) \prod_{n=1}^{M-1} f(\mathbf{x}_n | \mathbf{x}_{n-1}; \theta)$$

In the above equation  $f(\mathbf{x}_n | \mathbf{x}_{n-1}; \theta)$  represents the conditional probability (transition density) of observing  $\mathbf{x}_n$  given the observation  $\mathbf{x}_{n-1}$ . In practice, one usually takes a finite sample of data and presents this data to a Monte Carlo scheme that is meant to approximate the integral in equation 4.1 and finds the parameter values that yield the maximum value. In what follows, the function below is referred to as the log likelihood function (assume throughout that  $\mathbf{x}_0$  has a Dirac distribution) :

$$\mathcal{L} := \frac{1}{M} \sum_{i=1}^M \log(f(\mathbf{x}_i | \mathbf{x}_{i-1}))$$

Under our assumptions one has <sup>9</sup> the following:

$$\sqrt{(M)}(\theta - \hat{\theta}) \xrightarrow{\mathbb{P}_{\hat{\theta}}} N(0, \mathcal{F}^{-1})$$

Where in the above  $\hat{\theta}$  is the “true” parameter of the model;  $\theta$  represents the parameter estimated with a finite time series of length  $M$ ;  $\xrightarrow{\mathbb{P}_{\hat{\theta}}}$  denotes convergence in distribution [45, 22] under  $\mathbb{P}_{\hat{\theta}}$ ;  $N(0, \mathcal{F}^{-1})$  denotes a normal distribution with mean vector zero and covariance  $\mathcal{F}^{-1}$ . For a correctly specified model,  $\mathcal{F}$ <sup>10</sup> can be estimated in a variety of ways [47, 36]. Various conditions can be tested to see if asymptotic results are relevant for the finite sample sizes used [45, 36]. In this article sample sizes are moderate, but good agreement with some classical asymptotic predictions [47] is observed. When a closed-form transition density is in hand one can deterministically calculate  $\mathcal{F}$  in the stationary ergodic case <sup>11</sup>.

In practice, maximum likelihood does fail spectacularly for some simple models because of singularities that can be observed with the log likelihood function <sup>12</sup>. The

<sup>9</sup>This actually holds under less stringent regularity assumptions [45]

<sup>10</sup>I will adhere to common convention and call this the Fisher information matrix

<sup>11</sup>In the stationary ergodic case, if one has a time series  $(\mathbf{x}_1, \dots, \mathbf{x}_M)$  then one can ignore the initial distribution in the “infinite  $M$ ” limit. If the state is  $n$ -dimensional, then one can approximate the Fisher information by a  $2 \times n$  dimensional deterministic integral  $\left( \mathcal{F} \approx \int \frac{\partial \log(f(\mathbf{x} | \mathbf{x}_o; \hat{\theta}))}{\partial \theta} \frac{\partial \log(f(\mathbf{x} | \mathbf{x}_o; \hat{\theta}))}{\partial \theta}^T f(\mathbf{x} | \mathbf{x}_o; \hat{\theta}) dx d\pi(\mathbf{x}_o) \right)$ , where  $d\pi(\mathbf{x}_o)$  is the invariant distribution of model (which in the scalar case can usually be readily calculated in closed-form from the coefficients of the parametric SDE [24]). The difficulties encountered in the nonstationary time series situation is analogous to the situation of using the Metropolis algorithm to sample phase space [17]; in principle a deterministic integral could be evaluated, but with current computational power quadrature is not possible due to the high dimensionality of the problem

<sup>12</sup>Recall this term implies a finite sample size approximation to equation 4.1

classical example is the following: one assumes that a distribution is a mixture two Gaussians whose variance  $\in (0, \infty)$ . Then the finite sample MLE fails to exist in this simple case (see [7, 45] for a more in depth discussion)<sup>13</sup>.

The aforementioned point brings us to an important observation contained in this paper. It is well known that the transition density associated with a diffusion SDE can be solved through a corresponding PDE (via the Kolmogorov equations [3]). One can often prove that the density of the process has the regularity properties needed to make *exact* MLE successful (*a priori* regularity bounds associated with the log likelihood function is trickier) via techniques of harmonic analysis [41], but many useful properties determined by analytic techniques are only applicable to the *exact* transition density. Approximations to the transition density are needed in cases where the transition density is not available in closed-form. The approximations provided by Aït-Sahalia's Hermite expansion [2, 3] are useful for obtaining point parameter estimates, can capture the curvature of the transition density enough to approximate parameter distributions, and are sometimes accurate enough to create test statistics needed for some hypothesis tests. However, when one uses derivatives of the expansion for creating Wald or Rao<sup>14</sup> test statistics [7] it can introduce spurious singularities which complicates squeezing all of the information that is theoretically possible from MLE. I use the "Euler" estimator as a crude transition density approximation to demonstrate some points in this paper<sup>15</sup>. It is well known that the Euler estimator is biased [38], this fact helped to initiate a flood of transition density approximations in recent years [2, 3, 4, 6, 18, 42] (just to mention a few).

**4.2. Optimal Binary Alternative Hypothesis Testing: The Neyman-Pearson Lemma.** In this section it is assumed that one has a data set and two parameter vectors. Assume that one parameter vector is the "null hypothesis" and the other parameter vector is the "alternative". The type I error probability is defined as the probability of rejecting the null hypothesis when in fact the null is true (classically denoted by  $\alpha$ ). The power of a test against the alternative is the probability of rejecting the null hypothesis when in fact the alternative is true. An optimal test statistic can be found which for a specified  $\alpha$  maximizes the power [7]. To create the test statistic define the likelihood ratio by  $L := \frac{f(\mathbf{x}; \theta_{Alt})}{f(\mathbf{x}; \theta_{Null})}$ ;

one rejects the null if  $L > \beta^{NP}$  where  $\beta^{NP}$  is a scalar value that allows the following equality  $\int_{L > \beta^{NP}} f(\mathbf{x}, \theta_{Null}) dx = \alpha$

In the context of multiscale systems computations, this test is really only practical for stationary ergodic distributions (or for order parameters that are trapped for the duration of a simulation in a local free energy minima), but it provides us with insight as to how well the transition density captures the ratio of nearby parameter points.

---

<sup>13</sup>In practice, one can partially remedy this situation by finding a local minima using a variant of the technique outlined in section 4.4, but the new comer to MLE should be aware that some failures of MLE [35] are not as easy to remedy, especially when one has data that does not come from the assumed parametric model class

<sup>14</sup>These test are concerned with using the Fisher Information matrix as a normalizing matrix used to create a  $\chi^2$  statistic. Both tests can be used to construct confidence ellipsoids around parameter estimates. [45, 22, 7]

<sup>15</sup>This estimator is motivated by the Euler SDE simulation path technique [28]. One assumes that for a given observation pair  $(\mathbf{x}_n, \mathbf{x}_{n+1})$  that a normal distribution can be used whose standard deviation is given by the diffusion coefficient evaluated at  $\mathbf{x}_n$  times the square root of the time between successive observations ( $\sqrt{\delta t}$ ) and the conditional mean is given by applying the deterministic Euler scheme to the drift coefficient

Applications shown later require a highly accurate approximation of the likelihood ratio.

**4.3. Goodness-of-fit and Model Misspecification.** It is possible to test if the log likelihood function is consistent with the proposed model structure by testing the following condition [47]:

$$\mathcal{F}_{Hessian} := \frac{\partial^2 \mathcal{L}}{\partial \theta^2} = -\mathcal{F}_{OP}$$

Where the Hessian is evaluated at  $\hat{\theta}$  and  $\mathcal{F}_{OP}$  is defined by:

$$\mathcal{F}_{OP} := \frac{1}{M} \sum_{i=1}^M \frac{\partial \log(f(x_i|x_{i-1}; \hat{\theta}))}{\partial \theta} \frac{\partial \log(f(x_i|x_{i-1}; \hat{\theta}))}{\partial \theta}^T$$

In the above, the superscript  $T$  denotes the transposition operation,  $\mathcal{F}_{OP}$  is the “outer product”. For correctly specified models, both  $\mathcal{F}_{OP}$  and  $-\mathcal{F}_{Hessian}$  [22] are valid estimates of  $\mathcal{F}$ . When a closed-form expansion is in hand these quantities are easily computable after the optimal parameter is located.

For real data it is overly optimistic to expect to be able to exactly parameterize the density of the process with a Euclidean parameter vector. However, in some situations it is meaningful to attempt to project the data onto the proposed model structure [8, 47] yielding a Quasi-Maximum Likelihood Estimator (QMLE). When the true density does not lie in the proposed structural model class, one can still maximize the integral in equation 4.1 yielding the estimator that minimizes the Kullbeck-Leibler distance [31, 40]. Under assumptions laid out in [47], this QMLE converges to a normal distribution in the infinite sample limit:

$$\sqrt{(M)}(\theta - \hat{\theta}) \xrightarrow{\mathbb{P}_{\hat{\theta}}} N(0, \mathcal{C})$$

The matrix  $\mathcal{C}$  ( $:= \mathcal{F}_{Hessian}^{-1} \mathcal{F}_{OP} \mathcal{F}_{Hessian}^{-1}$ ) replaces  $\mathcal{F}^{-1}$ . This fact can be used to test the goodness-of-fit given the data and the optimal parameter vector via the Rao or Wald test statistic [47, 7]. The methodology laid out in [47] is comprehensive and powerful, but in order to develop techniques which can be accessed by the diverse audience involved in multiscale modeling, algorithms available in standard packages/libraries (MATLAB, IMSL) are employed.

**4.4. Le Cam’s Method and Likelihood Ratio Expansions (LAQ).** Lucien Le Cam was a major contributor to a variety of important asymptotic statistics results [33, 34, 36]; one of his major contributions was concerned with Locally Asymptotic Quadratic (LAQ) expansions of the log likelihood ratio (llr). Denote the llr symbolically by  $\Lambda_{h,M}(\theta)$ . It is given (for discrete Markovian models) by:

$$\Lambda_{h,M}(\theta) = \mathcal{L}_{\theta+\delta_M h} - \mathcal{L}_{\theta}$$

Here  $M$  is again the length of the times series ;  $h$  is a vector perturbation with the same dimensionality as  $\theta$ ;  $\delta_M$  is a matrix that scales the perturbation and  $\mathcal{L}_{\theta}$  denotes the llr evaluated at  $\theta$ ; for later use let  $h_M := \delta_M h$ . When the assumptions behind LAQ hold [26, 36], one can asymptotically approximate the above random variable by a normal limit experiment <sup>16</sup>. If one is in a neighborhood of the true parameter

<sup>16</sup>see [45, 36] for a clear introduction to this topic, consult [26] for an application to time series analysis

(denote the true parameter by  $\hat{\theta}$  and let  $\tilde{\theta}$  be contained in a  $\delta_M$  – neighborhood of  $\hat{\theta}$  ) the LAQ conditions imply

$$\Lambda_{h,M}(\hat{\theta}) - (h_M^T W_M(\hat{\theta}) - \frac{1}{2} h_M^T S_M(\hat{\theta}) h_M)$$

converges (in  $P_{\hat{\theta}}$  probability) to 0. In the above expressions, when  $\Lambda_{h,M}(\theta)$  is twice differentiable with respect to  $\theta$ ,  $S_M(\theta)$  and  $W_M(\theta)$  play the role of the first and second derivatives of the llr [26]<sup>17</sup> with respect to the parameter vector.

The contiguity condition is a generalization of the concept of absolute continuity [21]; it allows one to determine the distribution of “nearby” experiments which is sometimes useful for constructing hypothesis tests. If contiguity exists in the experiment, it [45] implies the following limit distribution:

$$(4.3) \quad \Lambda_{h,M}(\tilde{\theta}) \xrightarrow{\mathbb{P}_{\tilde{\theta}}} N\left(-\frac{1}{2} h_M^T S_M(\tilde{\theta}) h_M, h_M^T S_M(\tilde{\theta}) h_M\right)$$

The llr is of interest in asymptotic statistics because it provides a method for taking a classical parametric model and producing a scalar random variable which has the above limit distribution in the LAQ case (the practical utility of this theory is realized if the above normal distribution can still be used to reliably approximate the more complicated distribution of the llr of the proposed parametric model for finite sample sizes [34] ).

There are many other deep implications of LAQ, the method is only used in this paper to quantify the uncertainty associated with a nonergodic time series. In the stationary ergodic case the matrix  $W_M(\hat{\theta})$  coincides with deterministic quantity  $\mathcal{F}$  shown earlier, for nonergodic models the matrix is itself a random variable. I repeat the construction in Le Cam chapter 6 [36] here in order to show how one uses the llr in order to estimate  $W_M(\hat{\theta})$  (which can be used to roughly approximate the variance of the limit parameter distribution). To simplify the situation, assume that one is already within a  $\delta_M$  neighborhood of  $\hat{\theta}$  (this neighborhood is centered at  $\hat{\theta}$  ) and set the matrix  $\delta_M = \frac{1}{\sqrt{M}} Id$  where  $Id$  is the identity matrix. Suppose  $\theta \in \mathbb{R}^k$ , then one takes a basis set of  $\mathbb{R}^k$  (denote this set by  $\{b_1, \dots, b_k\}$ ) and evaluates:

$$\Lambda_{h,M}(\tilde{\theta} + \delta_M(b_i + b_j))$$

for  $i, j = 1, \dots, k$ ; the components of  $W_M(\tilde{\theta})$  are estimated by

$$(4.4) \quad W_M(\tilde{\theta})_{ij} \approx \frac{-[\Lambda_{h,M}(\tilde{\theta} + \delta_M(b_i + b_j)) - \Lambda_{h,M}(\tilde{\theta} + \delta_M(b_i)) - \Lambda_{h,M}(\tilde{\theta} + \delta_M(b_j))]}{b_i b_j}$$

Under the LAQ assumptions, one can claim that  $W_M(\tilde{\theta}) \xrightarrow{\mathbb{P}_{\tilde{\theta}}} W_M(\hat{\theta})$  as  $M$  tends to infinity . The theory shown here (developed by Le Cam) is purely an asymptotic one, however if one observes that the relation in equation 4.3 holds, it gives one more confidence when equation 4.4 is employed to approximate the quadratic expansion of the llr. In the situation where  $W_M(\hat{\theta})$  is random (as it will be in some of the

---

<sup>17</sup>this view is convenient for giving an intuitive interpretation of the above, but a classical Taylor expansion of  $\Lambda_{h,M}(\tilde{\theta})$  may fail to exist; however the LAQ “derivative” can still be defined

applications presented), one needs to repeat this procedure for a variety of paths <sup>18</sup> and then take expectations in order to get a rough estimate of the asymptotic parameter distributions. The numerical methods that use the LAQ expansions are purely heuristic, the theory developed above is proved in great detail for independent random variables; rigorous asymptotic statements about the llr associated with Markov chains are harder to make [34, 43]. The potential applications of these types of ideas in multiscale applications are merely shown via numerical results in this paper.

**5. Local Polynomial Diffusion Models.** Thus far, the main concern has been approximating the transition density and quantifying the goodness-of-fit of our simple models to the data. For the remainder of this section assume that the data can adequately be described by some arbitrary nonlinear effective SDE. Recall, I am working under the assumption that even if the true underlying potential energy surface is rugged, a smooth model of the drift and diffusion coefficients can be used to reliably approximate certain features of the free energy surface. In statistical mechanics, sometimes a limit theory exists for what the large sample system's effective dynamics converge to [19]. Unfortunately, for many interesting systems, the functional form of the drift and diffusion coefficients are completely unknown. Our research group has used the label "equation free methods" [27] to describe a set of numerical procedures that have been designed to deal with a situation where one has a simulation protocol that is believed to contain useful information and the information in the simulation is believed to be describable by an effective equation (with smooth coefficients), but the equation is unavailable in closed form. The early versions of this procedure used least squares approximation in order to get derivative information. Within the last couple of years, our group has extended the estimation procedure to match local linear SDE models (both vector and scalar) to the output of simulation data. The parametric models proposed are of the type given in equation 3.4. MLE and QMLE are greatly facilitated by the deterministic likelihood expansions developed by Aït-Sahalia [1, 2, 4] <sup>19</sup>.

Conceptually, I am just taking advantage of the fact that the accurate Aït-Sahalia Hermite expansion allows us to generalize the piecewise-polynomial (pp) concept to diffusion SDE models. Since I posit the existence of a smooth underlying effective diffusion model, the drift and diffusion coefficient functions are fit locally to linear models. One is free to use a fairly broad class of polynomials in the scalar case with a variant of Aït-Sahalia's expansion [4], but our future work is concerned with applying the techniques in this paper to the vector case. In that situation, a higher order polynomial of unknown vector functions is not practical from an estimation standpoint. Our experience has shown that if one wants to accurately capture the mean reversion portion of a nonlinear effective model that it usually becomes necessary to model the state dependence of the noise (this point is illustrated in section 6.5). In statistical terms, I am simply just finding the QMLE estimate of the parametric model shown in equation 3.4. However a variety of practical questions arise:

---

<sup>18</sup>In practice one may not have enough paths from an atomistic simulation to realize asymptotic statistics results. If a diffusion model is truly valid, one is always free to use the parameters obtained from a "small" sample in order to simulate additional paths [28], then use "bootstrap" techniques [45]

<sup>19</sup>Deterministic expansions are useful because one can quickly carry out parameter optimization and can easily evaluate the functionals needed to carry out variations of MLE in situations where MLE fails [36, 26]. Another obvious advantage is that in the case of stationary ergodic distributions one can easily carry out a quadrature and determine the asymptotic parameter distributions in situations where the parameter distributions converge to a normal random variable

- How does one determine if the estimated model is meaningful?
- In the case where an approximate transition density is used to estimate parameters, how sensitive is the QMLE projection to the quality of the approximation?
- How does one choose the size of the neighborhood where a local linear model is valid?
- How does one piece together the local models in order to create a global nonlinear effective diffusion model?

The first issue is readily handled by the theory discussed earlier. The second issue is concerned with semiparametric estimation and robust statistics. These are important and active area of research in statistics [8, 45] (and in the future could make great contributions to multiscale modeling), but results are currently difficult (for this author) to translate into practical and reliable numerical methods associated with the ideas laid out here. In section 4.1 it is shown that the true model is not too sensitive to “contaminated data” and this quality is retained by the expansions of Aït-Sahalia, however is not by the overly crude Euler estimator.

The method proposed is well-equipped to handle the third issue. The method requires the user to obtain a batch of trajectories from a simulation. In order to carry out a classical estimation procedure, one must create a partition of state space where a local linear diffusion model is an accurate representation of the underlying nonlinear diffusion (see figure 5.1). Once the data set is collected, one is free to make as many partitions as desired. The simple idea is to only present observation pairs  $(\mathbf{x}_n, \mathbf{x}_{n+1})$  to the log likelihood function that have “ $\mathbf{x}_n$ ” within the selected neighborhood. The neighborhood size must be chosen to be small enough that the QMLE parameters estimates of the pp SDE model are statistically meaningful <sup>20</sup> and large enough to contain enough samples to obtain the desired parameter accuracy (and have asymptotic results hold). The main difficulty that the method faces is determining a neighborhood yielding a satisfactory compromise between the two aforementioned factors. This procedure is greatly facilitated by the equations of a limit process if one is known. Otherwise one must use numerical experimentation to attempt to determine how smooth the underlying coefficients functions are (recall the assumption that a simple low dimensional model exists). In multiscale modeling we have the convenience of controlling the initial conditions of the (assumed meaningful) atomistic simulation making this type of pp SDE modelling more practical (otherwise one can only estimate parameters around state points visited frequently by the sample path). Note that this method makes the time series length itself a random variable. In addition, many applications of this idea lead to estimation of a nonstationary time series. It has already been noted earlier that it is computationally difficult to calculate the Fisher information matrix in these circumstances. These facts indicate that the LAQ likelihood ratio approximation might be useful. It should be noted that optimal tests rarely exist in this type of situation, however in the estimation literature some heuristic techniques have been recommended [5, 16]. The technical details of these methods require some fairly specialized arguments and due to this author’s ignorance of both recent developments and the more important aspects of the theory, goodness-of-fit tests are avoided in this situation <sup>21</sup>.

---

<sup>20</sup>The goodness-of-fit techniques presented in the previous section can check this, however in practice this procedure greatly benefits from modern nonparametric techniques [24, 11]

<sup>21</sup>Before proceeding, I would like to explicitly point out that if one has an initial distribution of

In regards to the final item, I merely present two simplistic methods of piecing together our local models in section 5. I also demonstrate that the LAQ expansion can give a useful quantification of parameter uncertainty for our toy models. The information contained in an LAQ approximation can be used in more sophisticated “matching” schemes. Again this area is well outside of this author’s research area; if the problem at hand is of any real significance one should consult [10, 15, 46] for modern matching techniques, but at some stage one will almost certainly have to appeal to some form of heuristics (a.k.a., “the art of numerical computation”).

**5.1. Relevance to Multiscale Numerical Methods.** The details of the tools used may obscure their utility in multiscale modeling, so the connection is summarized here. The computational load to carry out a full simulation is too great, so a diffusion approximation is made which hopes to capture the relevant information in the underlying model. Goodness-of-fit tests are needed to quantify the quality of the approximation. If the model is found to be statistically acceptable, then one would be interested in the confidence intervals associated with the estimate. Different state points have different levels of noise; having a reliable method for theoretically predicting parameter uncertainty as a function of sample size at different state points can assist one in designing “efficient experiments” because one can allocate computational resources in an intelligent manor. QMLE is a nice tool for achieving all these tasks, however it can fail if it is followed “verbatim”, especially when one uses an approximation of the transition density. Estimators based on llr methods are appealing in situations where standard QMLE fails because they are applicable to a wider class of problems and the distribution of the llr asymptotically converges to a manageable distribution for certain model classes [34].

**6. Results and Discussion.** In order to get MLE (QMLE) parameter estimates in all of the section to follow, the IMSL Nelder-Mead search algorithm is employed using the termination criterion of  $5 \times 10^{-8}$  with an initial parameter distribution dictated by a uniform distribution around the slightly biased (+10%) true parameter values in the cases of known or approximately known models and from an assumed limit process in the final application.

**6.1. Maximum Likelihood Estimation Results.** Tables 6.1 and 6.2 report the empirically measured mean and standard deviation of the parameter distributions as well as the asymptotic predictions for the standard deviation for situation I A-D and situation I A-C (using data spaced  $\delta t = 2^{-5}, 2^{-3}$  units respectively). We see that as  $\beta$  increases the estimated mean reversion parameter decreases in magnitude. This makes sense because the parametric model in equation 3.3 assumes a single free energy minimum; as the magnitude of the sine wave added to the potential increases, one experiences a situation where the “well-depths” associated with the local minima of the glassy potential increase, retarding the rate of mean reversion. The exact magnitude of this affect depends heavily on several factors, some of which are: the size of the noise amplitude compared to that of the mean reversion rate (which corresponds to the smooth part of the drift), the frequency of the sine wave’s perturbation, the amplitude of the sine wave, and the sampling frequency. The last two effects are

---

points clustered near each other initially and as time proceeds the ensemble mean slowly “funnels” its way down to global or local minima, then the problem is slightly easier because one only needs to determine the boundary of the “right hand end points” of the collection of time series. The point stressed is that data only needs to be collected *once* and a statistically analyzed on or off-line (the deterministic expansions of Aït-Sahalia make the former a possibility)

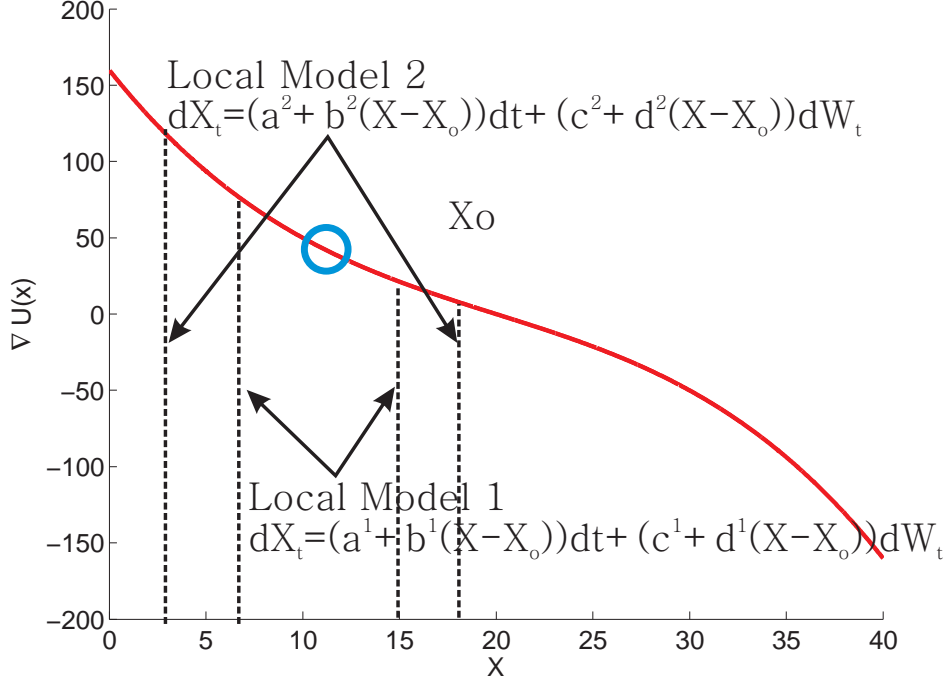


FIG. 5.1. *LAQ Screening Method Illustration* Graphical illustration of LAQ screening method for Situation II B. The circle corresponds to a state point where a parametric model was obtained using that particular " $X_o$ ". For smooth models the quality of the linear approximation depends on the neighborhood size of both the drift and diffusion approximation (not shown). Once the data is collected, one is free to vary  $X_o$  and/or the neighborhood size.

quantified in tables 6.1 and 6.2. Inspection of these tables shows that the when the true density is used, the effective model estimated from the data is relatively independent of the sampling frequency. Note that as the observation frequency decreases the quality of the expansion (in time) naturally decreases, but even for relatively "large" times between samples Aït-Sahalia's expansion remains accurate. The quality of the Euler expansion is very sensitive to the time between samples and it introduces a bias even when the "perfect data" is presented to the estimator. I continue to show the results for the Euler estimator despite these shortcomings because in section 6.4 the estimator demonstrates a redeeming quality which can be used in conjunction with the transition density estimator of Aït-Sahalia in situations where the latter fails. The tables also show that the sample size is large enough to partially realize asymptotic results in most cases. Table 6.3 shows similar results; the cubic perturbation introduced into the drift of the situation II results in a higher mean reversion rate. In section 6.4 it is demonstrated that if one presents "windowed" data (those observation pairs that fall within a small neighborhood centered around the estimated  $\alpha$  parameter) that the bias introduced by the nonlinear drift perturbation steadily decreases in magnitude as the window size decreases which intuitively makes sense given our assumptions. Unfortunately, this simple procedure creates a more complicated statistical problem in regards to theoretical parameter distribution predictions because

TABLE 6.1

**Situation I Parameter Distributions** The data used to obtain the parameter distributions was  $N = 2000$  sample paths of an SDE sampled over  $M = 4000$  time intervals evenly spaced at  $\delta t = 2^{-5}$  taken from the invariant distribution of an Euler path simulation. The empirical mean and standard deviation of the parameter distributions are reported as well as the asymptotic predictions of the standard deviation are reported. For correctly specified models (case A) the asymptotic standard deviation given by  $\mathcal{F}_{OP}$  (calculable by a deterministic integral) and for misspecified models the standard deviation predicted by  $\mathcal{C}$  is given

| Scenario/<br>Expansion Method | $\langle \alpha \rangle$ | $\langle \kappa \rangle$ | $\langle \sigma \rangle$ | $\sigma_\alpha^{\text{Asymp}}$ | $\sigma_\kappa^{\text{Asymp}}$ | $\sigma_\sigma^{\text{Asymp}}$ |
|-------------------------------|--------------------------|--------------------------|--------------------------|--------------------------------|--------------------------------|--------------------------------|
|                               |                          |                          |                          | $\sigma_\alpha^{\text{Emp}}$   | $\sigma_\kappa^{\text{Emp}}$   | $\sigma_\sigma^{\text{Emp}}$   |
| Sit I A<br>True               | 20.0052                  | 4.0428                   | 4.0168                   | 0.40026                        | 0.26975                        | 0.047621                       |
|                               |                          |                          |                          | 0.40152                        | 0.27501                        | 0.047197                       |
| Sit I A<br>Ait-Sahalia        | 20.0454                  | 3.9628                   | 4.0159                   | 0.39938                        | 0.25999                        | 0.047575                       |
|                               |                          |                          |                          | 0.40249                        | 0.26681                        | 0.047197                       |
| Sit I A<br>Euler              | 20.0052                  | 3.7961                   | 3.7869                   | 0.40000                        | 0.25298                        | 0.044722                       |
|                               |                          |                          |                          | 0.40146                        | 0.24439                        | 0.042119                       |
| Sit I B<br>True               | 19.9985                  | 4.0148                   | 4.0102                   | 0.40089                        | 0.27011                        | 0.047769                       |
|                               |                          |                          |                          | 0.39973                        | 0.26831                        | 0.045601                       |
| Sit I B<br>Ait-Sahalia        | 20.0374                  | 3.9362                   | 4.0093                   | 0.3956                         | 0.24097                        | 0.047761                       |
|                               |                          |                          |                          | 0.40102                        | 0.26296                        | 0.045592                       |
| Sit I B<br>Euler              | 19.9985                  | 3.7707                   | 3.7822                   | 0.40097                        | 0.23932                        | 0.042992                       |
|                               |                          |                          |                          | 0.40052                        | 0.23995                        | 0.041049                       |
| Sit I C<br>True               | 19.8675                  | 3.7844                   | 3.9277                   | 0.41654                        | 0.26111                        | 0.047758                       |
|                               |                          |                          |                          | 0.41787                        | 0.27209                        | 0.047093                       |
| Sit I C<br>Ait-Sahalia        | 19.9016                  | 3.7085                   | 3.9267                   | 0.41061                        | 0.23487                        | 0.047743                       |
|                               |                          |                          |                          | 0.4196                         | 0.27554                        | 0.047109                       |
| Sit I C<br>Euler              | 19.8674                  | 3.5374                   | 3.7195                   | 0.42007                        | 0.2335                         | 0.043175                       |
|                               |                          |                          |                          | 0.41835                        | 0.24537                        | 0.041998                       |
| Sit I D<br>True               | 19.3406                  | 2.9368                   | 3.581                    | 0.49515                        | 0.22916                        | 0.047533                       |
|                               |                          |                          |                          | 0.48422                        | 0.27015                        | 0.058569                       |
| Sit I D<br>Ait-Sahalia        | 19.3614                  | 2.8953                   | 3.5787                   | 0.48505                        | 0.21071                        | 0.047373                       |
|                               |                          |                          |                          | 0.48679                        | 0.26281                        | 0.050485                       |
| Sit I D<br>Euler              | 19.3387                  | 2.6775                   | 3.4387                   | 0.51899                        | 0.21057                        | 0.0439                         |
|                               |                          |                          |                          | 0.48306                        | 0.24238                        | 0.044822                       |

a deterministic approximation of the parameter distribution is much harder to get using this technique.

**6.2. Optimal Binary Alternative Hypothesis Testing Results.** In figure 6.1, the top/right axis corresponds to the Neyman-Pearson critical value versus the theoretical type I error probability for all three transition density expansions using the null as the true (known) parameters of situation II A and the alternative as the QMLE parameters obtained using situation II B data with the exact CIR density. The left/bottom axis shows the analytically calculated cumulative distribution of rejecting the null under the alternative using the three different transition densities (plugging in the same alternative parameters estimated by QMLE) as well as the empirically measured distribution of the likelihood ratio (see caption for additional details). We see that the sample size is large enough to realize agreement between the measured and limit distributions. The expansion of Ait-Sahalia provides a very close estimate of this distribution, whereas the distribution predicted by the Euler approximation deviates substantially.

**6.3. Goodness-of-fit and Model Misspecification Results.** Here it is demonstrated how the various transition densities perform when one tries to use them to evaluate the derivatives needed to estimate the asymptotic QMLE parameter vari-

TABLE 6.2

**Situation I Parameter Distributions** Same information as table 6.1 except the time intervals are evenly spaced at  $\delta t = 2^{-3}$ . Note how the parameter distribution quality degrades (as compared to table 6.1), this is due in part to the failure of the transition density expansion (as evident from situation I A). Another thing to note is that when the true CIR density is used, the parameters estimated are relatively independent of the sampling frequency (which is a very desirable quality). This is not the case for the two transition density expansions, however the magnitude of the discrepancy between this table and the previous is much smaller for the Aït-Sahalia expansion.

| Scenario/<br>Expansion Method | $\langle \alpha \rangle$ | $\langle \kappa \rangle$ | $\langle \sigma \rangle$ | $\sigma_\alpha^{\text{Asymp}}$ | $\sigma_\kappa^{\text{Asymp}}$ | $\sigma_\sigma^{\text{Asymp}}$ |
|-------------------------------|--------------------------|--------------------------|--------------------------|--------------------------------|--------------------------------|--------------------------------|
|                               |                          |                          |                          | $\sigma_\alpha^{\text{Emp}}$   | $\sigma_\kappa^{\text{Emp}}$   | $\sigma_\sigma^{\text{Emp}}$   |
| Sit I A<br>True               | 19.9996                  | 4.0296                   | 4.019                    | 0.20206                        | 0.16652                        | 0.056847                       |
|                               |                          |                          |                          | 0.20085                        | 0.16673                        | 0.057301                       |
| Sit I A<br>Aït-Sahalia        | 20.1162                  | 3.6394                   | 3.9971                   | 0.18208                        | 0.10863                        | 0.055179                       |
|                               |                          |                          |                          | 0.22812                        | 0.23505                        | 0.06125                        |
| Sit I A<br>Euler              | 19.9996                  | 3.1652                   | 3.2323                   | 0.20088                        | 0.12692                        | 0.045736                       |
|                               |                          |                          |                          | 0.20088                        | 0.10329                        | 0.038508                       |
| Sit I B<br>True               | 19.9915                  | 4.0095                   | 4.0123                   | 0.7049                         | 0.4502                         | 0.03758                        |
|                               |                          |                          |                          | 0.20131                        | 0.1659                         | 0.056841                       |
| Sit I B<br>Aït-Sahalia        | 20.118                   | 3.6523                   | 3.9941                   | 0.76493                        | 0.41996                        | 0.037335                       |
|                               |                          |                          |                          | 0.22589                        | 0.21442                        | 0.059281                       |
| Sit I B<br>Euler              | 19.9915                  | 3.1517                   | 3.2306                   | 0.30418                        | 0.26104                        | 0.049705                       |
|                               |                          |                          |                          | 0.20138                        | 0.10267                        | 0.038656                       |
| Sit I C<br>True               | 19.8718                  | 3.7377                   | 3.9093                   | 0.32825                        | 0.29782                        | 0.048524                       |
|                               |                          |                          |                          | 0.20573                        | 0.16222                        | 0.055943                       |
| Sit I C<br>Aït-Sahalia        | 19.9835                  | 3.4578                   | 3.8975                   | 0.33702                        | 0.26354                        | 0.041954                       |
|                               |                          |                          |                          | 0.22621                        | 0.21599                        | 0.05993                        |
| Sit I C<br>Euler              | 19.8717                  | 2.9659                   | 3.1967                   | 0.38195                        | 0.24293                        | 0.04877                        |
|                               |                          |                          |                          | 0.20574                        | 0.10375                        | 0.03815                        |

TABLE 6.3

**Situation II Parameter Distributions** Same information as table 6.1 except  $M = 4500$ .

| Scenario/<br>Expansion Method | $\langle \alpha \rangle$ | $\langle \kappa \rangle$ | $\langle \sigma \rangle$ | $\sigma_\alpha^{\text{Asymp}}$ | $\sigma_\kappa^{\text{Asymp}}$ | $\sigma_\sigma^{\text{Asymp}}$ |
|-------------------------------|--------------------------|--------------------------|--------------------------|--------------------------------|--------------------------------|--------------------------------|
|                               |                          |                          |                          | $\sigma_\alpha^{\text{Emp}}$   | $\sigma_\kappa^{\text{Emp}}$   | $\sigma_\sigma^{\text{Emp}}$   |
| Sit II A<br>True              | 19.9877                  | 4.0512                   | 4.0169                   | 0.37737                        | 0.25432                        | 0.044898                       |
|                               |                          |                          |                          | 0.38691                        | 0.26327                        | 0.04653                        |
| Sit II A<br>Aït-Sahalia       | 20.0272                  | 3.9695                   | 4.0159                   | 0.37654                        | 0.24512                        | 0.044854                       |
|                               |                          |                          |                          | 0.38803                        | 0.25535                        | 0.046481                       |
| Sit II A<br>Euler             | 19.988                   | 3.8045                   | 3.7862                   | 0.37712                        | 0.23852                        | 0.042164                       |
|                               |                          |                          |                          | 0.38732                        | 0.23417                        | 0.041944                       |
| Sit II B<br>True              | 19.826                   | 4.9256                   | 4.018                    | 0.30542                        | 0.28151                        | 0.045772                       |
|                               |                          |                          |                          | 0.31247                        | 0.26417                        | 0.047077                       |
| Sit II B<br>Aït-Sahalia       | 19.8544                  | 4.8679                   | 4.0186                   | 0.29819                        | 0.25567                        | 0.045828                       |
|                               |                          |                          |                          | 0.30856                        | 0.25292                        | 0.047127                       |
| Sit II B<br>Euler             | 19.826                   | 4.5645                   | 3.7382                   | 0.30545                        | 0.24273                        | 0.039965                       |
|                               |                          |                          |                          | 0.31238                        | 0.22756                        | 0.040756                       |

ance shown in [47]. Before proceeding, a mildly problematic aspect of the expansion of Aït-Sahalia is pointed out. To illustrate the problem, the histograms of  $\frac{\partial^2 \mathcal{L}}{\partial \alpha^2}$  are plotted for 500 sample paths using the three expansions. The particular histogram shown using the Aït-Sahalia expansion had 25 observations that were disregarded because of unusually high values in the calculated quantities. The expansion of Aït-Sahalia is very accurate, but its functional derivatives can unfortunately introduce spurious singularities into the transition density approximation. To show a specific

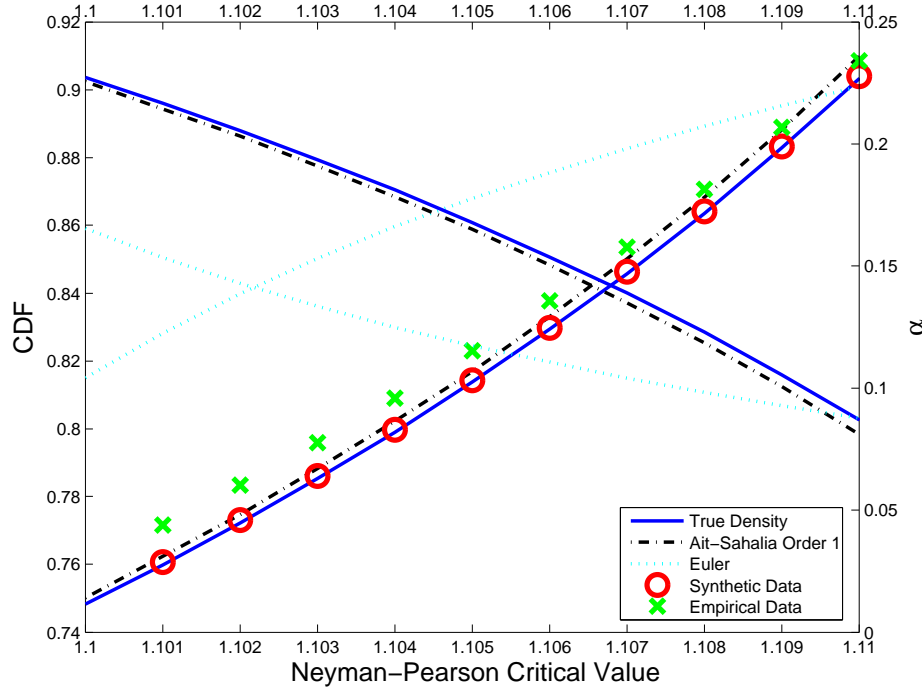


FIG. 6.1. *Neyman-Pearson Results* The Neyman-Pearson test carried out on situation II B data using the QMLE parameter estimate as the alternative and the exact (known) parameters associated with situation II A as the null. The curves represent the deterministic calculation of the type I error probability as a function of the critical value (right axis) and the theoretical CDF of the likelihood ratio obtained by using the various transition density expansions assuming ergodic sampling of the invariant distribution (left axis). The “x’s” correspond to using the actual situation II B data (nonlinear potential) and the “o’s” correspond to the distribution of the likelihood ratio obtained using the QMLE parameters estimated to simulate sample paths of the structural model proposed (plugging in the average of the QMLE parameter distribution) and then using the exact CIR density to evaluate the likelihood ratio.

example of this, take the logarithm of the order one Aït-Sahalia CIR expansion <sup>22</sup> and calculate the second derivative with respect to  $\alpha$  and plug in the observation pair (obtained via an Euler path simulation)  $[x_n, x_{n-1}] = [3.1826960, 3.305275]$  and set  $\sigma = 4, \kappa = 4, \delta t = 2^{-5}$ . The bottom panel in figure 6.2 plots the resulting function of  $\alpha$ . For the particular model and parameter values shown, this type of situation is only encountered when calculating functional derivatives. In the “heuristic” part of this paper, sample values where singularities are hit when evaluating the pure log likelihood function are encountered. The classic method of dealing with this is to apply a one-step MLE estimator <sup>23</sup>. A minor modification of Le Cam’s method shown in section

<sup>22</sup>Mathematica code available from <http://www.princeton.edu/~yacine/research.htm>

<sup>23</sup>The basic ideas of these procedures is to use a simple restricted parameter set that is “rich” in the parameter space [8]. An example of this would be to take a discrete mesh of parameter space and optimize the log likelihood over this finite set, then carry out a few more iterations refining the mesh slightly each time. The main idea is to keep the parameter values away from singularities associated with the finite sample log likelihood. Refer to the literature on asymptotically centering estimators

4.4 provides one possible construction of a one-step MLE estimator. Many one-step methods require a parameter guess that is within a “reasonable neighborhood” of the true parameter value (the exact size of the neighborhood can be chosen using an approximation of the Fisher information matrix). Table 6.4 illustrates that if one starts with a slightly perturbed guess of the true parameter that Le Cam’s method can get fairly close to the true parameter vector if the transition density approximation is very accurate (the likelihood ratio expansion was obtained from situation II A data and the one-step used is outlined in Le Cam [36] chapter 6). The asymptotic likelihood expansions are extremely valuable in parametric estimation; unfortunately this application requires an extremely accurate transition density approximation <sup>24</sup>. Throughout this paper the first order (in time) Aït-Sahalia expansion have been used; only in table 6.4 do I report results from a higher order expansion (order four). Recall in section 6.1 that the order one Aït-Sahalia expansion provided an accurate approximation of the likelihood ratio for a simple hypothesis test. The test statistic generated for the Neyman-Pearson test only required the ratio of one observation pair at two nearby parameter vectors. The transition density expansion does introduce a systematic bias into the approximation, and the nature the bias does exhibit a smooth dependence on the parameter values making the ratio of two nearby probability densities also exhibit a significant bias and these small errors accumulate as the time series length grows complicating matters. Some techniques and analysis have already been developed for approximating the LAQ expansion of random variables in the case where the density is not known explicitly [26]; most techniques developed require one to empirically measure the transition density. For stochastic processes, the empirical distribution techniques are mildly inconvenient (from a computational standpoint) because one needs to determine an empirical density approximation for each observation pair.

Now let us return to the goodness-of-fit issue. First, the condition  $\mathcal{F}_{Hessian} = -\mathcal{F}_{OP}$  is tested. If the condition holds  $T := \sum_{i,j=1}^k \mathcal{F}_{Hessian}^{ij} + \mathcal{F}_{OP}^{ij}$  should be a mean zero random variable (the superscripts denote matrix components and  $k$  is the number of parameters estimated). If it is assumed that the classical central limit theorem (CLT) holds and that the sample sizes used are large enough to appeal to the CLT and approximate the sample mean by a normal distribution of unknown variance, then the classical t-test can be employed [7] (more sophisticated tests are proposed in [47]). Figure 6.3 plots the t-test results for testing if  $\mathcal{F}_{Hessian} = -\mathcal{F}_{OP}$  for various sample sizes (the Aït-Sahalia data is screened by the technique mentioned in footnote 24). For lower sample sizes (path number), one can confidently claim that the mean is nonzero when using the true transition density or the Aït-Sahalia (the Euler results are not plotted). The figure also shows that as the number of paths grows (with the time series length held fixed), it becomes easier to detect discrepancies between the data and the assumed model. Even when the true transition density is used

---

in [36, 33] for another example of a one-step method.

<sup>24</sup>Instead of applying one-step methods (a full discussion would slightly overload this paper and distract from the simpler points), in the simple parametric models studied I remedy the singularity issue by using the Euler approximation to determine when a singularity is hit. It is possible to distinguish between spurious singularities from log likelihood function singularities in the CIR case because the true transition density is known. In all of the CIR applications the singularities hit were in fact spurious. I simply threw out sample paths where the absolute value of the logarithm of the transition density of the Aït-Sahalia expansion differed from that of the Euler approximation by a factor of three anywhere along the discretely observed path (this occurred less than 4% in the CIR studies, in the SSA studies this number increased to roughly 25%).

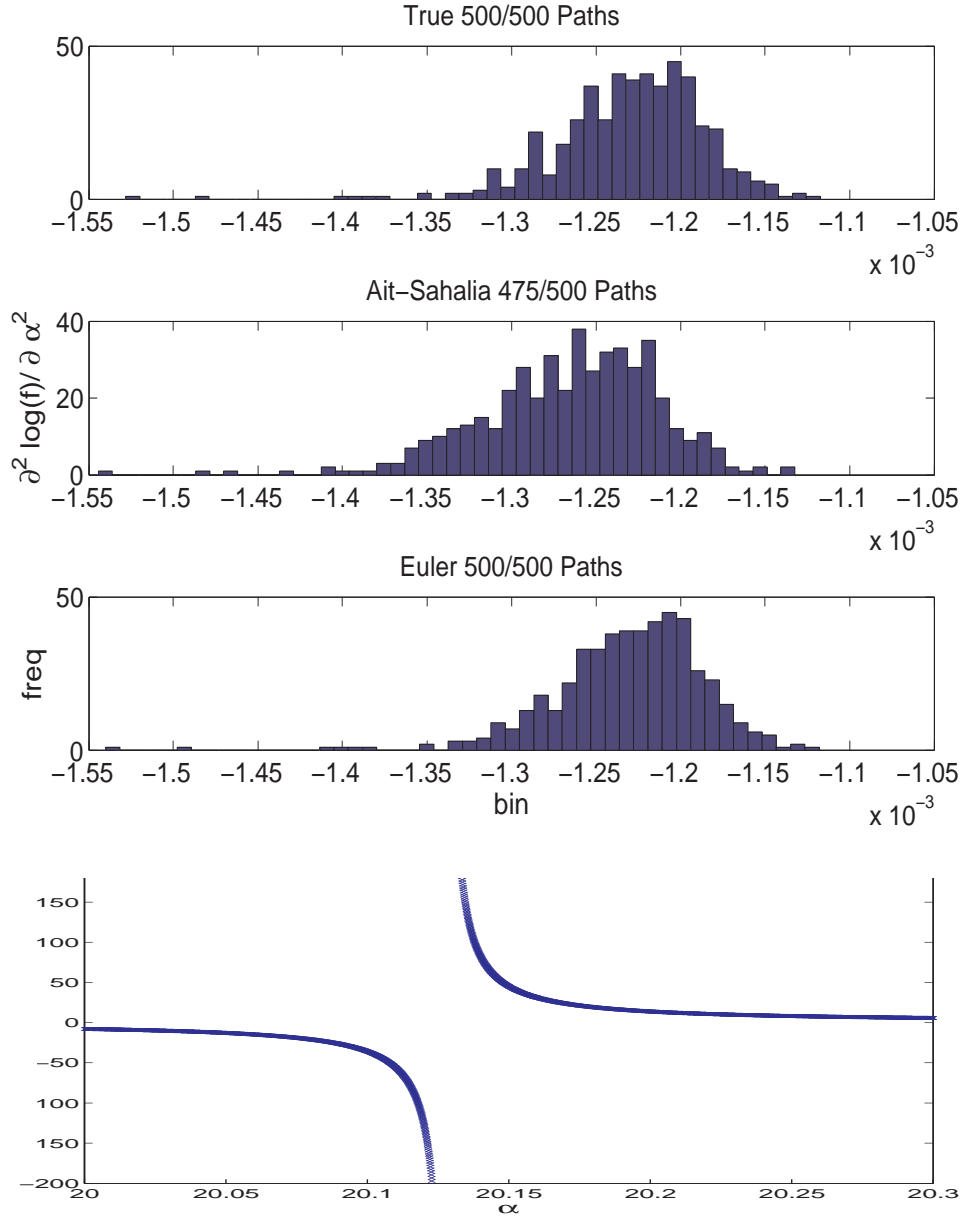


FIG. 6.2. *Histogram of diagonal components of  $\mathcal{F}_{\text{Hessian}}$  corresponding to  $\alpha$  for the three transition density expansions*. The histograms all differ slightly in shape indicating that the curvature of the three transition densities differs slightly (data taken from situation I C with  $\delta t = 2^{-5}$ ). In the second plot 25 observations were thrown out because there were outliers caused by spurious singularities in the transition density expansion. The bottom panel gives one demonstration of how the Ait-Sahalia expansion can introduce spurious singularities into the log-likelihood function. The data shown is the second derivative of transition density with respect to  $\alpha$  as a function of  $\alpha$  for a particular observation (see text for discussion). The fat tails of the log likelihood function make a simple screening of outliers (caused by spurious singularities) very difficult if one does not have the true transition density to reference.

TABLE 6.4

**Le Cam LAQ One-Step Test** The data used was situation II A with  $\delta t = 2^{-5}$ . The LAQ motivated one-step expansion was carried out at the point  $\theta = (20.1, 4.5, 4.1)$ , consult Le Cam [36] chapter 6 for details. The one-step estimate of the parameter results from adding the quantity below to  $\theta$ . This type of procedure is necessary when standard MLE misbehaves (in our study the exact transition density behaves nicely, but the Aït-Sahalia expansion misbehaves because of singularities introduced into the expansion). The table shows that the LAQ update gets one close to the true parameter when an extremely accurate approximation of the transition density is in hand. The Aït-Sahalia order one and Euler updates are not as good, but still usable. The major problem with these estimators is that the contiguity condition becomes difficult to verify (a condition that needs to be met before the LAQ expansion can be used with confidence). The last two columns display -2 times the mean and the variance of the likelihood ratio measured by evaluating the llr at  $\hat{\theta}$  and  $\hat{\theta} + h_M$  where  $h_M = (1.2, 0, 0.12)$ . In the infinite sample limit these two quantities will be identical (assuming  $h_M$  is continually scaled properly). For the exact and order four Aït-Sahalia expansion one observes close results. For the other two expansions this is not the case (see text for further discussion).

| Expansion           | $\Delta\alpha$ | $\Delta\kappa$ | $\Delta\gamma$ | $-2\mu_{\Lambda_{\theta\text{true}}}$ | $\sigma_{\Lambda_{\theta\text{true}}}$ |
|---------------------|----------------|----------------|----------------|---------------------------------------|----------------------------------------|
| CIR Exact           | -0.9507        | -0.4791        | -0.0931        | 12.9402                               | 13.8679                                |
| Aït-Sahalia Order 4 | -0.9507        | -0.4791        | -0.0931        | 12.9405                               | 13.8679                                |
| Aït-Sahalia Order 1 | -1.0065        | -0.7499        | -0.1208        | 13.6013                               | 39.0793                                |
| Euler               | -0.9621        | -0.7344        | -0.3156        | 41.8144                               | 16.0470                                |

with the correct model, one observes that as sample size increases (in paths) that it becomes easier to reject the null. This is because the equality  $\mathcal{F}_{\text{Hessian}} = -\mathcal{F}_{OP}$  is an asymptotic result. A finite size time series can *never* fully realize asymptotic results; as more paths are analyzed the departure from the limit becomes easier to detect. One should also note that as the number of paths increases it also becomes easier to detect the errors in the transition density expansion. Before proceeding to check for model misspecification in the presence of an approximated transition density, one should determine if asymptotic results are valid for “perfect data” using the same time series length, then proceed to check the accuracy of the expansion by some MC tests (like the ones presented in the previous section).

For extreme cases (situation I C and D) the t-test safely rejects the null for small sizes (see figure 6.3 and the inset). This indicates that the data is well outside the particular structural model class under study, but one can still test if the asymptotic QMLE results hold. Figure 6.4 plots the exact probability density of the  $\chi^2(3)$  random variable as well a test statistic given in [47] (which will be denoted by  $\mathcal{HW}$ <sup>25</sup>) We see that both the approximation and the exact transition density appear close to the predicted limit distribution indicating that the asymptotic results approximately hold for the sample sizes used. I quantitatively compare how well the empirical distributions match the limit distribution by using the Kolmogorov-Smirnov (KS) test with various sample sizes in the inset of figure 6.4<sup>26</sup>. The average p-value is

<sup>25</sup>  $\mathcal{HW} := Mg(\theta) \left[ \nabla g(\theta) \mathcal{C}_{(\theta)} \nabla g(\theta)^T \right]^{-1} g(\theta)^T$  where  $g(\cdot)$  is the gradient of the log likelihood function. If  $\theta \in \mathbb{R}^k$  then under conditions stated in [47] this random variable converges in distribution to  $\chi^2(k)^2$  random variable. This statistic was originally proposed by Halbert White [47].

<sup>26</sup> In this particular application we are still significantly away from the limit distribution. The sample sizes used for estimation are large enough that a test as powerful as the KS would reject equality of the two distributions with very high certainty if one used all of the data at hand. For this reason I only present portions of the data to the KS test. In many interesting atomistic simulation studies, one can only afford to generate a couple hundred sample paths making this type of goodness-of-fit test useful in practice. An alternative would be to partition the CDF into bins and use the  $\chi^2$  square goodness-of-fit test [37].

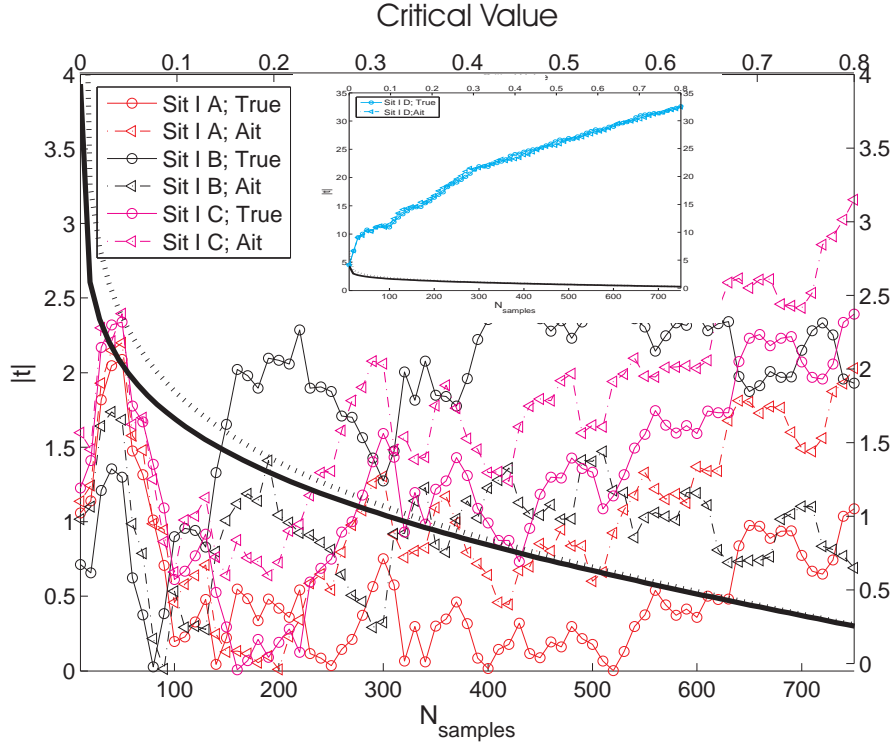


FIG. 6.3. *Model Misspecification t-test Results* The left/bottom axis plots the t-statistic obtained by summing the components of  $\mathcal{F}_{OP}$  and  $\mathcal{F}_{Hessian}$  for various sample sizes (time series length is fixed, different  $N_{samples}$  values correspond to using different sample path numbers to create the random variables required to generate the sample mean and standard deviation needed for the t-test). The right/top axis is to be used with the lines without marks; the top axis is the critical value (cv) of the t-test (lowest  $|t|$  needed to reject the null for a given  $\alpha$ ). The solid line corresponds to the theoretical cv of a sample size =375 and the dashed line corresponds to a sample size =10. The inset plots the situation I D test which can be rejected quickly with high confidence.

obtained by applying the one sample KS test [7] using 500 draws of size  $N_{samples}$  from the pool of  $\mathcal{H}W$  random variables associated with the  $N_{samples}$  paths using the  $\chi^2(3)$  density as the null (sampling with replacement). The result of this procedure is shown in the inset of figure 6.4. We see that the test statistic created using the Aït-Sahalia expansion is rejected before that associated with the true density indicating the possibility that the errors in the expansion cause a *mildly* inflated rejection rate in situation I C.

**6.4. Le Cam's Method and Likelihood Ratio Expansions Results.** Table 6.5 presents parameter estimates of the “windowed” data (the window size used is given in the captions) from situation II B. We see that as the window size decreases the estimator mean moves closer to that of the “uncontaminated” model but the variance of the estimator increases. I use Le Cam's LAQ expansion with the Aït-Sahalia transition density expansions in order to quantify the uncertainty in the measurement. One should observe that the LAQ matrix is closely related to the variance of the parameter distributions (for a more precise description of the connection consult

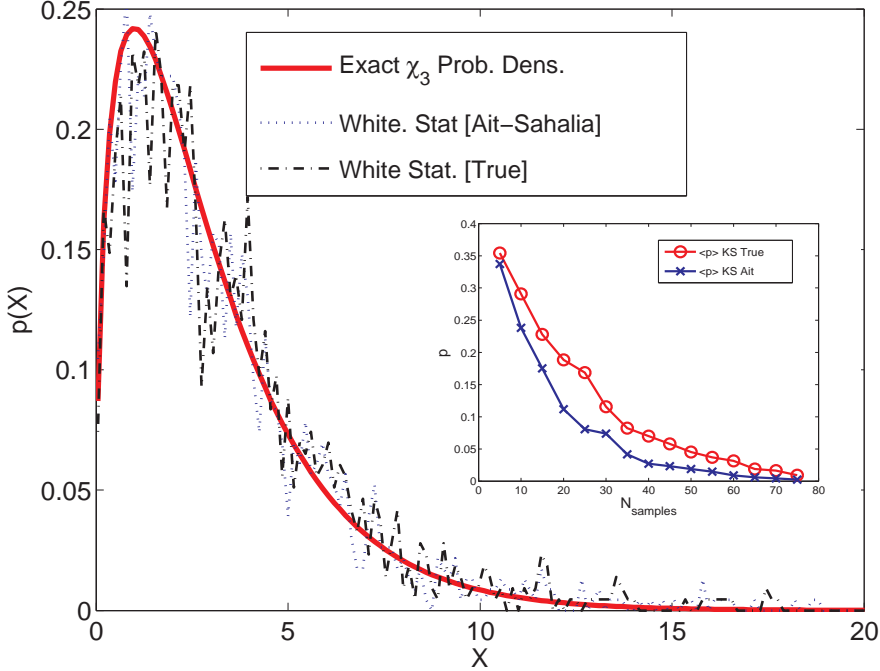


FIG. 6.4. *Goodness-of-Fit with Kolmogorov-Smirnov Test* The  $\chi^2(3)$  probability density is plotted along with the empirical distribution of the test-statistic proposed in [47] for situation I C. The inset shows a plot of the p-value (minimum  $\alpha$  needed to reject the null given the data) obtained using the one-sample Kolmogorov-Smirnov test versus the number of paths used to create the test statistic. If the full set of samples were used, the test would have no problem in rejecting the null. This is due to the fact that asymptotic results are never truly realized with finite sample sizes. The plot illustrates that the test statistic generated by the Ait-Sahalia expansion does faithfully capture the average curvature of the log likelihood function in a misspecified model.

[26, 5]). The agreement between the estimated parameter variance is not as sharp as it was in the case of a stationary distribution, but there one had the convenience of evaluating a deterministic integral (in situation A). Furthermore the asymptotic results are harder to realize because some observation pairs are not used to obtain parameter estimates (due to the windowing). If one has a situation where the window size is small enough to give ‘‘meaningful’’ QMLE parameter estimates and the number of observation pairs is large enough to appeal to asymptotic methods, then the LAQ ‘‘screening’’ method can be used to define a cost function which can be used to intelligently choose the window size.

**6.5. Local Polynomial Diffusion Models Results .** In the first application, the pp SDE method is applied to data generated by the unperturbed CIR model ( $\gamma = \beta = 0$ ); I pretend that the functional form of the drift or diffusion coefficient is unknown. Five arbitrary state points denoted by  $\{E_i\}_{i=1,5}$  (shown as circles in figure 6.5) are chosen and the parameters of the affine SDE model shown in equation 3.4 are obtained there. The LAQ expansion is used in order to obtain parameter uncertainty estimates and the results are compared to the empirical parameter distribution

TABLE 6.5

**Situation II B Parameter Distributions with LAQ Screening** The data used to obtain the parameter distributions was the same as that used in table 6.3 except here only results of using the Ait-Sahalia expansion are presented using “windowed” data. The base point ( $X_o$ ) of all of the expansion shown below is 20 which corresponds to the true  $\alpha$  parameter and the interval used to filter the data is given in the first left column. The empirical mean and standard deviation of the parameters are given along with the LAQ prediction of the parameter uncertainty.

| Window   | $\langle \alpha \rangle$ | $\langle \kappa \rangle$ | $\langle \sigma \rangle$ | $\sigma_\alpha^{\text{Asymp}}$ | $\sigma_\alpha^{\text{Asymp}}$ | $\sigma_\kappa^{\text{Asymp}}$ |
|----------|--------------------------|--------------------------|--------------------------|--------------------------------|--------------------------------|--------------------------------|
|          |                          |                          |                          | $\sigma_\alpha^{\text{Emp}}$   | $\sigma_\kappa^{\text{Emp}}$   | $\sigma_\sigma^{\text{Emp}}$   |
| (16, 24) | 19.993                   | 4.080                    | 4.006                    | 0.577                          | 1.079                          | 0.094                          |
|          |                          |                          |                          | 0.560                          | 1.008                          | 0.085                          |
| (15, 25) | 20.047                   | 4.228                    | 4.003                    | 0.502                          | 0.780                          | 0.078                          |
|          |                          |                          |                          | 0.530                          | 0.802                          | 0.078                          |
| (14, 26) | 20.021                   | 4.365                    | 4.006                    | 0.450                          | 0.629                          | 0.068                          |
|          |                          |                          |                          | 0.474                          | 0.627                          | 0.066                          |

TABLE 6.6

**Piecewise Polynomial SDE Parameter Distributions of Situation II B** The data used to obtain the parameter distributions was  $N = 2000$  sample paths of an SDE sampled over  $M = 4000$  time intervals evenly spaced at  $\delta t = 2^{-5}$  using expansion point  $X_o$  with the window size given in the second column. The empirical mean and standard deviation of the parameter distributions are reported as well as the LAQ predictions of the standard deviation.

| Xo   | Window       | $\langle a \rangle$ | $\langle b \rangle$ | $\langle c \rangle$ | $\langle d \rangle$ | $\sigma_a^{\text{Asymp}}$ | $\sigma_b^{\text{Asymp}}$ | $\sigma_c^{\text{Asymp}}$ | $\sigma_d^{\text{Asymp}}$ |
|------|--------------|---------------------|---------------------|---------------------|---------------------|---------------------------|---------------------------|---------------------------|---------------------------|
|      |              |                     |                     |                     |                     | $\sigma_a^{\text{Emp}}$   | $\sigma_b^{\text{Emp}}$   | $\sigma_c^{\text{Emp}}$   | $\sigma_d^{\text{Emp}}$   |
| 16   | (11, 22)     | 15.909              | -4.227              | 15.600              | 0.534               | 1.939                     | 0.696                     | 0.295                     | 0.067                     |
|      |              |                     |                     |                     |                     | 1.999                     | 0.713                     | 0.278                     | 0.061                     |
| 18   | (13, 25)     | 8.226               | -4.118              | 16.987              | 0.462               | 1.898                     | 0.6344                    | 0.288                     | 0.061                     |
|      |              |                     |                     |                     |                     | 1.984                     | 0.667                     | 0.293                     | 0.062                     |
| 20   | (16, 24)     | -0.021              | -3.879              | 17.862              | 0.437               | 2.408                     | 1.131                     | 0.425                     | 0.085                     |
|      |              |                     |                     |                     |                     | 2.419                     | 1.157                     | 0.43774                   | 0.088                     |
| 22.5 | (15.5, 29.5) | -9.994              | -4.064              | 18.971              | 0.435               | 2.284                     | 0.624                     | 0.334                     | 0.058                     |
|      |              |                     |                     |                     |                     | 2.490                     | 0.615                     | 0.338                     | 0.0848                    |
| 25   | (21, 29)     | -20.602             | -4.050              | 19.982              | 0.391               | 3.310                     | 1.092                     | 0.514                     | 0.091                     |
|      |              |                     |                     |                     |                     | 3.648                     | 1.426                     | 0.598                     | 0.105                     |

measured by carrying out QMLE on the “screened” data in table 6.6 .

At this point we have in hand, estimates of the constant and linear sensitivities of the coefficients of the SDE. The entire function in the range shown can be approximated by the following interpolation procedure:

$$f_j(x) = \frac{w^L f_j^L(x) + w^R f_j^R(x)}{Z}$$

where  $j = 1, 2$  corresponds to the drift and diffusion coefficients respectively,  $w^L$  and  $w^R$  are the weights associated with the left and right expansion point,  $f_j^L(x)$  is the affine approximation to the nonlinear function based on the closest expansion point whose value is less than or equal to  $x$  (similarly for  $f_j^R(x)$ , but use the nearest expansion point strictly greater than  $x$ ). The weights were assigned by the *ad hoc* rule:

$$w^L(x) = \frac{(\sigma_C + \sigma_D(x)(x - E_i))^{-1} (E_{i+1} - x)}{E_{i+1} - E_i}$$

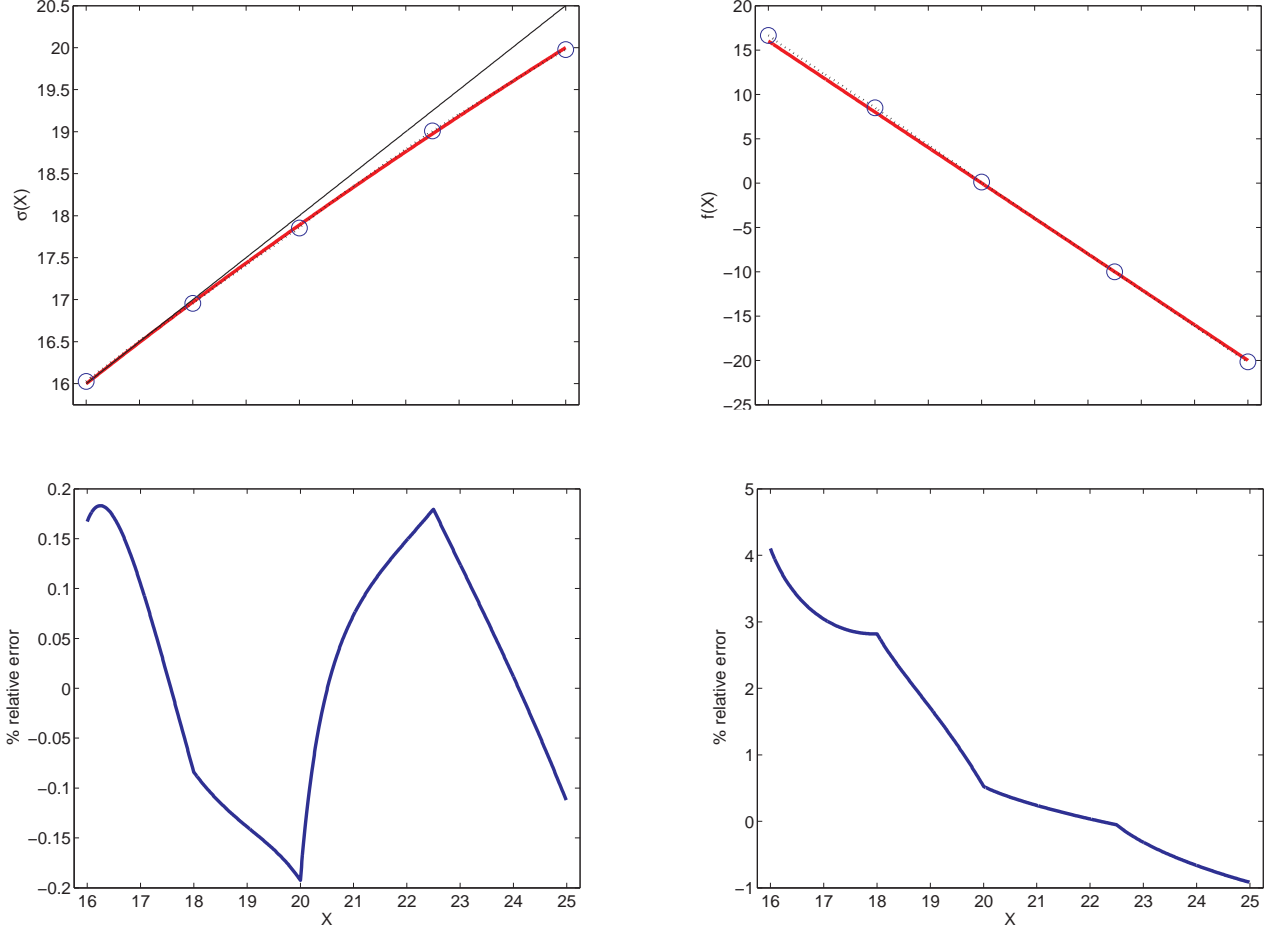


FIG. 6.5. *Piecewise Polynomial Approximation of CIR Model* The top panels plot the diffusion (left) and drift (right) function obtained by the interpolation procedure given in section 6.5. The top left panel plots the first order Taylor expansion (evaluated at  $X_o = 16$ ) of the diffusion coefficient from the known function to show how much the true function deviates from linearity and how well our procedure detects this change. The bottom figures plot the corresponding relative errors (using the exact known SDE coefficient functions). See text in section 6.5 for discussion on systematic vs. random errors.

$$w^R(x) = \frac{(\sigma_C + \sigma_D(x)(E_{i+1} - x))^{-1} (x - E_i)}{E_{i+1} - E_i}$$

$$Z = w^L + w^R$$

The results of this simple interpolation procedure are shown as a dotted line in figure 6.5 (in the rule above,  $\sigma_C$  and  $\sigma_D$  are the empirically measured parameter standard deviations of the constant and linear term of the diffusion term; the interpolation rule for the drift is analogous). Figure 6.5 plots the relative error of using this procedure using the known SDE coefficient functions as the “truth”. The errors

in the diffusion coefficient function do not indicate a systematic bias in contrast to the drift coefficient <sup>27</sup>.

In the final application, the parameters of the model are unknown. The parameter were obtained with the LAQ screening technique. The SSA process was run until  $N$  sample paths reached an approximately invariant distributions. Then  $N = 200$  paths were used to obtain initial parameter estimates; for expansion points in the tails of the invariant distribution an additional  $N = 600$  paths were simulated in order to get sharper estimates of the poorly sampled state points <sup>28</sup>. Here a smoothing B-spline [10] was used (specifically MATLAB's spaps function) to piece together the constants  $(a, c)$  of the local models in order to smoothly interpolate between state points. Each point was given the same weight when creating the spline, the LAQ technique for measuring parameter uncertainty could be used to give different weights to the measured parameters, but this procedure was not carried out here because the inherent jump nature of the data complicates matters slightly <sup>29</sup>. The information contained in the linear coefficients  $(b, d)$  was not used for interpolation purposes because the variance of the parameter of the linear terms was much larger than those of the constant terms in the case studied. However, if one ignores the linear terms in the local model the constants estimated are significantly affected (see figure 6.6). One observes significant departure of the SSA model parameters from the limiting drift function (plotted as a dashed red line). The number of particles in the SSA system was increased to  $2 \times 10^6$  and the parameters of the effective model in the drift were estimated and demonstrate that the limiting drift function is measured with the estimators used (see inset in figure 6.6). As the system size increases, the noise decreases, limiting the state points visited (hence the drift function estimated does not cover as large as a range as the first SSA case considered). The estimated diffusion function in figure 6.6 demonstrates dependence on the transition density used (Aït-Sahalia order one and Euler). In this application the Ornstein-Uhlenbeck (OU) transition density was used to demonstrate the importance of accounting for state dependent noise (note the systematic difference in the constant noise parameter estimated using that the three

---

<sup>27</sup>I offer an intuitive explanation for this fact; if one *naively assumes* that the true paths come from an Euler simulation with Euler step sizes corresponding to the observation frequency then one is in the “Gaussian case”. In between expansion points, the Taylor expansion of the known diffusion function consistently over estimates the diffusion function at nearby points (the diffusion coefficient is concave). The *true* transition density of the SDE has a smaller variance (the data generating process). When one uses the simple Euler density approximation in QMLE, the magnitude of the mean reversion parameter appears to be larger than it really is because of the error in the Taylor series approximation of the diffusion function (larger noise is expected making the deterministic trend appear stronger). The actual situation is much more complicated due to the fact that the distributions are not Gaussian, a complicated nonlinear function is used to obtain parameter estimates (QMLE), finite sampling effects, etc. However figure 6.5 is consistent with this overly simplified intuitive explanation.

<sup>28</sup>I initially optimized parameters over individual paths in order to estimate the parameter distribution variance. When parameter were optimized on a pathwise basis, a significant fraction ( $\approx 25\%$ ) of observation pairs resulted in *assumed* spurious singularities in the Aït-Sahalia expansion. To constrain the parameter space explored in the optimization, I found the QMLE parameters with *all* of the data (over time and paths). This helped prevent the optimization routine from attempting to evaluate the log likelihood function at parameter values that cause spurious singularities because the parameter space explored was reduced because the trial QMLE parameters needed to be good for all of the paths.

<sup>29</sup>In practice one could overcome this difficulty by obtaining the QMLE, generate SDE sample paths with the model parameters obtained, then find the LAQ parameter variance of a genuine diffusion. In applications where the uncertainty associated with using the local model technique on imperfect data is desired, the problem is much harder. One should consult the specialized literature [8, 43, 45] for guidance; this author can not make any sound general recommendations.

transition density estimators)

Figure 6.7 plots the invariant empirical CDF of the SSA data versus that predicted by a sample path simulation of our obtained nonlinear model (constructed from the B-spline interpolation of the estimated local SDE models). The inset plots the difference between the two empirical CDF's. Our interest in this application was in getting a parametric description of the invariant distribution, if the dynamics of the process are of more interest consult [11] for a useful test which is made possible if one has an approximation of the transition density.

**7. Conclusions and Outlook.** In this paper I have demonstrated that the expansions of Aït-Sahalia can potentially be a useful tool in the parametric estimation associated with computational studies of multiscale systems. Parameter estimates can accurately be obtained and the curvature of the model is accurately represented by the expansion in a variety of applications. These facts can be exploited to estimate parameter distributions and construct useful inference procedures. The overly simple Euler expansion behaves poorly in accuracy of the estimate and in the curvature of the transition density (as shown early on by Lo [38]), but it has the redeeming feature that it does not appear to introduce any spurious singularities into the transition density in the regimes studied here. In large sample statistics applications, point singularities can *usually* be remedied [33, 34, 36] by using likelihood ratio expansions. Unfortunately, many of these techniques require an extremely accurate estimate of the transition density. For imperfect transition densities with systematic errors this becomes mildly problematic<sup>30</sup>.

I have also demonstrated a heuristic method for locally approximating a non-trivial SDE by a collection of simple local models. The application was inspired by the need to accurately measure the parameters, quantify the uncertainty and determine the goodness-of-fit of parametric diffusion models around atomistic data. The piecewise SDE technique presented is simple in nature, but it raises many deep questions. Insight from the semiparametric, robust and large sample statistics communities would greatly assist in further developing this type of numerical method. The general method is appealing because it can be used to estimate complicated models where the underlying “signal of interest” obeys smooth evolution rules of unknown functional form. The resulting parametric model structure (which is typically a complicated function due to the “matching” used) can then be passed on to diffusion path simulation methods in order to generate additional data which can be used in order to construct confidence bands or carry out established inference procedures.

From a practical point of view it would be desirable to apply the techniques in this paper to Aït-Sahalia's method in the vector case because many interesting physical systems depend on a couple of “reaction coordinates” [25, 30, 13]. Unfortunately the vector version of the expansion usually requires one to use an additional Taylor series approximation (which increases the chance of spurious singularities and decreases the quality of the curvature estimate); this researcher has been able to use the expansions in order to get useful parameter estimates, but has not had as much success in pushing them as far as the scalar expansions. A numerical method which can be used in conjunction with the expansions of Aït-Sahalia in order to get detailed information about the likelihood ratio associated with smooth SDE's (diffusion and jump models) is currently being explored by the author.

---

<sup>30</sup>Methods proposed in [4] are applicable to a wider class of models and help the accuracy of the transition density expansion in the scalar case, but the vector case poses a more challenging problem

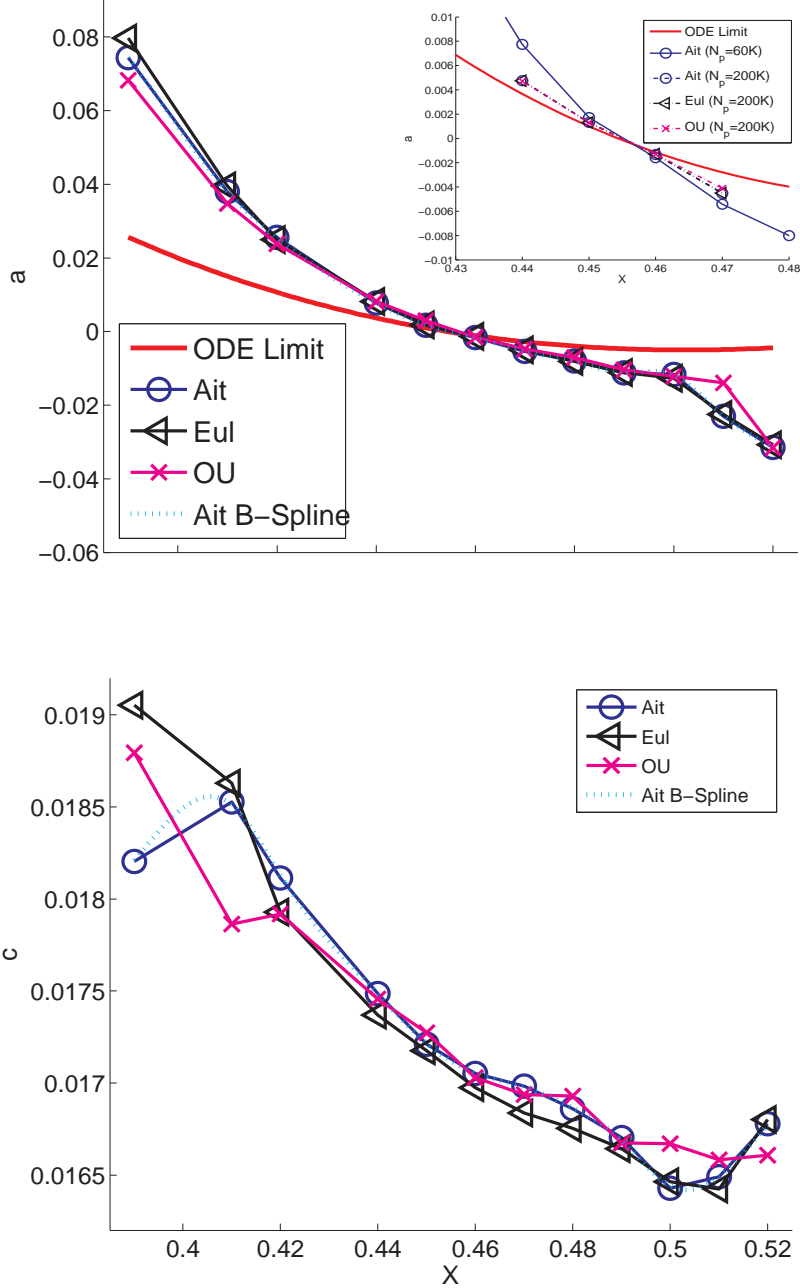


FIG. 6.6. *Estimated Nonlinear Drift (Global)* The LAQ “window” method was used to obtain the plots shown. The results of three different transition density estimates are shown (the OU model sets  $d$  in equation 3.4 equal to zero). The top panel contains the drift coefficient corresponding to a SSA simulation containing  $60^2$  particles. The thick solid line corresponds to infinite system size drift function. The dotted line corresponds to the B-spline of the Aït-Sahalia Expansion. The inset shows the drift coefficient corresponding to a SSA simulation containing  $2 \times 10^6$  particles. Observe how the drift function convergence towards the expected limit equation with moderate sample sizes, however for small particle systems the results are substantially different. The bottom panel displays the measured diffusion coefficient (the infinite sample limit has zero noise)

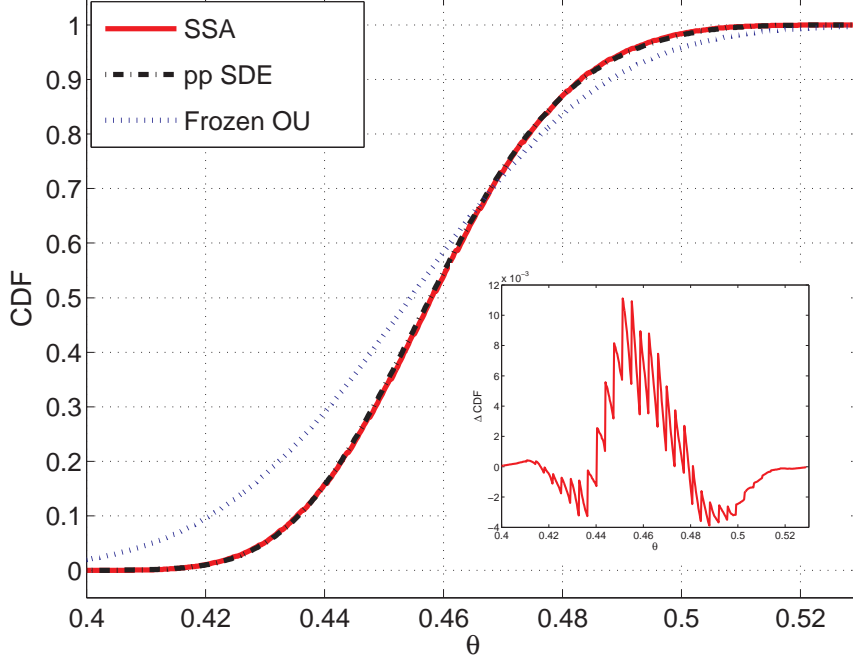


FIG. 6.7. *CDF and KS test* ( $N_{molecules} = 3600$ ) The CDF of the SSA invariant distribution (empirically measured) plotted against that of the piecewise-polynomial (pp) local SDE model (simulated by long time Euler integration [28]). In addition the invariant distribution of the OU model obtained is plotted (the model parameters of the local OU model were measured at the state point where the drift is zero). This was done to show what effect neglecting the nonlinear drift and state dependent diffusion has on the equilibrium CDF. The inset plots the difference between the invariant distribution CDF of the SSA data and that of the pp SDE model.

**8. Acknowledgements.** The author would like to thank Ioannis Kevrekidis and Adam Meadows for comments and advise and Yacine Aït-Sahalia for providing help with the transition density expansions.

#### REFERENCES

- [1] Y. AÏT-SAHALIA, *Transition densities for interest rate and other nonlinear diffusions*, Journal of Finance, 54 (1999), pp. 1361–1395.
- [2] ———, *Closed-form likelihood expansions for multivariate diffusions*, Technical Report, (2001).
- [3] ———, *Maximum-likelihood estimation of discretely-sampled diffusions: A closed-form approximation approach*, Econometrica, 70 (2002), pp. 223–262.
- [4] G. BAKSHI AND J. NENGJIU, *A refinement to aït-sahalia's (2002) "maximum likelihood estimation of discretely sampled diffusions: A closed-form approximation approach*.
- [5] I. BASAWA AND D.J. SCOTT, *Asymptotic Optimal Inference for Non-Ergodic Models*, Springer-Verlag, 1983.
- [6] B.M. BIBBY AND M. SØRENSEN, *Martingale estimation functions for discretely observed diffusion processes*, 1 (1995), pp. 17–39.
- [7] P. J. BICKEL AND K.J. DOKSUM, *Mathematical Statistics: Basic Ideas and Selected Topics*, Prentice Hall, Upper Saddle River, NJ, 2001.
- [8] P. J. BICKEL, C. A. J. KLAASSEN, Y. RITOV, AND J. A. WELLNER, *Efficient and Adaptive*

*Estimation for Semiparametric Models*, Johns Hopkins University Press, Baltimore, 1993.

[9] R.A. CURTIS AND M.W. DEEM, *A statistical mechanics study of ring size, ring shape, and the relation to pores found in zeolites*, J. Phys. Chem. B, (2003), pp. 8612–8620.

[10] C. DE BOOR, *A practical guide to splines*, Springer, New York, 2001.

[11] F.X. DIEBOLD, T. GUNTHER, AND A. TAY, *evaluating density forecasts with applications to financial risk management*, International Economic Review, (1998), pp. 863–883.

[12] D.J. EARL AND M.W. DEEM, *Optimal allocation of replicas to processors in parallel tempering simulations*, J. Phys. Chem. B, (2004), pp. 6844–6849.

[13] B. ENSING, A. LAIO, F.L. GERVASIO, M. PARRINELLO, AND M.L. KLEIN, *A minimum free energy reaction path for the e2 reaction between fluoro ethane and a fluoride ion*, 126 (2004), pp. 9492–9493.

[14] R. ERBAN, I.G. KEVREKIDIS, D. ADALSTEINSSON, AND T. ELSTON, *Gene regulatory networks: a coarse-grained, equation-free approach to multiscale computation*, Arxiv, (2005).

[15] J. FAN, *Nonlinear time series : nonparametric and parametric methods*, Springer, New York, 2003.

[16] P. FEIGIN, *Asymptotic theory of conditional inference for stochastic processes*, Stochastic Processes and their Applications, 22 (1986), pp. 89–102.

[17] D. FRENKEL AND B. SMIT, *Understanding Molecular Simulation: From Algorithms to Applications*, Academic-Press, 2002.

[18] A.R. GALLANT AND G. TAUCHEN, *Which moments to match?*, Econometric Theory, 12 (1996), pp. 657–681.

[19] G. GIACOMIN AND J.L. LEBOWITZ, *Phase segregation dynamics in particle system with long range interactions ii: interchange motion*, Siam J. Appl. Math., 58 (1998), pp. 1707–1729.

[20] D.T. GILLESPIE AND L.R. PETZOLD, *Improved lead-size selection for accelerated stochastic simulation*, Journal of Chemical Physics, 119 (2003).

[21] P.R. HALMOS AND L.J. SAVAGE, *Application of the Radon-Nikodym theorem to the theory of sufficient statistics*, The Annals of Mathematical Statistics, 20 (1949), pp. 225–241.

[22] J.D. HAMILTON, *Time Series Analysis*, Princeton University Press, 1994.

[23] C. HARDIN, M.P. EASTWOOD, M. PRENTISS, Z. LUTHEY-SCHULTEN, AND WOLYNES P.G., *Folding funnels: The key to robust protein structure prediction*.

[24] Y. HONG AND H. LI, *Nonparametric specification testing for continuous-time models with applications to term structure of interest rates*, The Review of Financial Studies, (2005), pp. 37–84.

[25] G. HUMMER AND I.G. KEVREKIDIS, *Coarse molecular dynamics of a peptide fragment: Free energy, kinetics, and long-time dynamics computations*, Journal of Chemical Physics, 118 (2003), pp. 10762–10773.

[26] P. JEGANATHAN, *Some aspects of asymptotic theory with applications to time series models*, Econometric Theory, 11 (1995), pp. 818–887.

[27] I.G. KEVREKIDIS, C.W. GEAR, AND G. HUMMER, *Equation-free: The computer-aided analysis of complex multiscale systems*, AIChE Journal, 50 (2004).

[28] P. KLOEDEN AND E. PLATEN, *Numerical Solution of Stochastic Differential Equations*, Springer-Verlag, 1992.

[29] D.I. KOPELEVICH, A.Z. PANAGIOTOPoulos, AND I.G. KEVREKIDIS, *Coarse-grained kinetic computations for rare events: Application to micelle formation*, Journal of Chemical Physics, 122 (2005), p. 044908.

[30] RUNBORG O. KRISHNAN, J. AND I. G. KEVREKIDIS, *Bifurcation analysis of nonlinear reaction-diffusion problems using wavelet-based reduction techniques*.

[31] S. KULLBACK AND R.A. LEIBLER, *On information and sufficiency*, The Annals of Mathematical Statistics, 22 (1951).

[32] E. LA NAVE, F. SCIORTINO, P TARTAGLIA, M.S. SHELL, AND P. G. DEBENEDETTI, *Test of non-equilibrium thermodynamics in glassy systems: the soft-sphere case*, Phys Rev. E, (2003), p. 032103.

[33] L. LE CAM, *Locally asymptotically normal families of distributions*, University of California Publications in Statistics, 3 (1960), pp. 37–98.

[34] ———, *Asymptotic Methods in Statistical Decision Theory*, Springer-Verlag, New York, 1986.

[35] ———, *Maximum likelihood: an introduction*, International Statistical Review, 58 (1990), pp. 153–172.

[36] L. LE CAM AND G. L. YANG, *Asymptotics in Statistics: Some Basic Concepts*, Springer-Verlag, 2000.

[37] E.L. LEHMANN, *Testing statistical hypotheses*, New York, 1959.

[38] H.W. LO, *Maximum likelihood estimation of generalized ito processes with discretely sampled data*, Econometric Theory, (1988), pp. 231–247.

- [39] A. MAKEEV, D. MAROUDAS, AND I. G. KEVREKIDIS, *Coarse bifurcation analysis of kinetic monte a lattice-gas model with lateral interactions*.
- [40] P.W. MILLAR, *The minimax principle in asymptotic decision theory*, Lecture Notes in Math., (1983), pp. 75–265.
- [41] D. NUALART, *The Malliavin Calculus and Related Topics*, Springer, New York, 1995.
- [42] A.R. PEDERSEN, *A new approach to maximum likelihood estimation for stochastic differential equations based on discrete observations*.
- [43] H. RIEDER, *Robust asymptotic statistics*, Springer-Verlag, New York, 1994.
- [44] E. SCHUTZ, N. HARTMANN, Y. KEVREKIDIS, AND R. IMBIHL, *Microchemical engineering of catalytic reactions*, Catalysis Letters, (1998), pp. 181–186.
- [45] A. VAN DER VAART, *Asymptotic Statistics*, Cambridge University Press, 1998.
- [46] G. WAHBA, *Spline models for observational data*, SIAM, Philadelphia, 1990.
- [47] H. WHITE, *Maximum likelihood estimation of misspecified models*, Econometrica, 50 (1982), pp. 1–25.